

1 Understanding biomass fractionation in subcritical & supercritical 2 water

3 María José Cocero*, Álvaro Cabeza, Nerea Abad, Tijana Adamovic, Luis Vaquerizo, Celia M.
4 Martínez, María Victoria Pazo-Cepeda.

5 *High Pressure Processes Group, Department of Chemical Engineering and Environmental*
6 *Technology, University of Valladolid (Spain). Doctor Mergelina s/n. 47011, Valladolid, Spain.*

7 * Corresponding author. Tel: +34 983423174; fax: +34 983423013.

8 *E-mail addresses: mjcocero@iq.uva.es*

9 Abstract

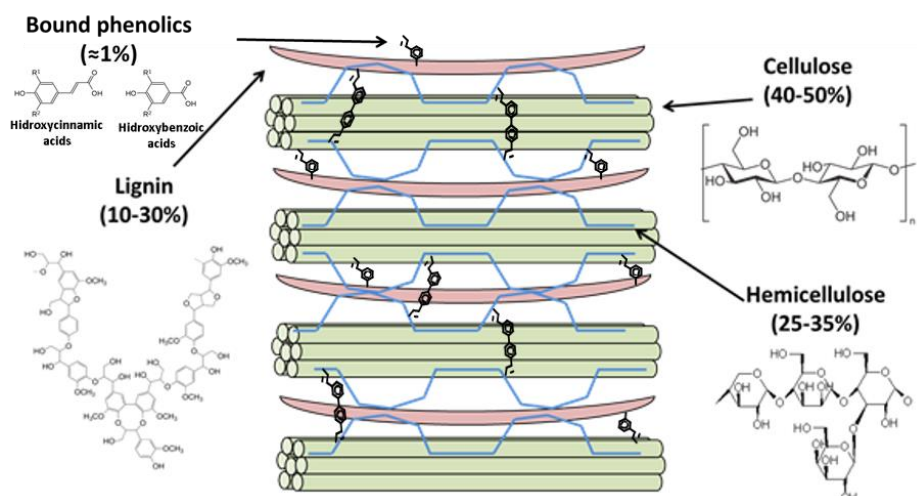
10 Biomass fractionation into its individual building blocks poses a major challenge
11 to the biorefinery concept. The recalcitrance of the lignocellulose matrix and the
12 high crystallinity of cellulose make typical feed stocks difficult to separate into
13 their components. Hydrothermal processing fractionates biomass by its
14 hydrolysis. However, a deep knowledge of hydrolysis principles is required since
15 an inappropriate selection of the operating parameters such as an excessive
16 temperature and a long residence times causes dramatic selectivity losses. This
17 review is divided in four main sections which present the fundamentals of
18 lignocellulosic biomass fractionation in hemicelluloses, cellulose and lignin. As
19 the biomass structure plays an important role, a section to study the extraction of
20 the linked phenols that joint lignin and hemicelluloses is included.

21 1. Introduction

22 Shifting the chemical industry away from petrochemical feedstocks towards
23 renewable, bio-based chemicals and materials is a long-term strategy of the
24 European Union. This “biorefinery” concept, despite being proposed as early as
25 the late 1980s, has still not come to fruition because the cost and complexity of
26 processing biomass to generate practical, usable, saleable feedstocks makes it
27 unfeasible.

28 Lignocellulose is the most abundant, cheapest and easiest grown form of
29 biomass, and it is composed of three main fractions: cellulose (40-50%),

30 hemicellulose (25-35%) and lignin (10-30%), in addition to minor compounds.
 31 These fractions represent potential feedstocks for bio-sourced commodity
 32 chemicals, but due do their differing chemical functionalities (lignin made up of
 33 linked aromatic units, hemicellulose of C5 sugars and cellulose of C6 sugars)
 34 separation steps are necessary to isolate the appropriate fraction and break it
 35 into its individual building blocks (e.g. sugars for cellulose/hemicellulose and
 36 aromatic units for lignin).
 37



38
 39
 40

Figure 1: Lignocellulosic biomass structure

41 This fractionation of biomass into its individual building blocks poses a major
 42 challenge to the biorefinery concept, because the recalcitrance of the
 43 lignocellulose matrix and high crystallinity of cellulose makes typical feedstocks
 44 difficult to separate into their components. For this reason, it typically requires
 45 long reaction times (from 30 minutes for the hydrothermal hydrolysis to 24-70
 46 hours for enzymatic hydrolysis) and the presence of strong reagents (sodium
 47 hydroxide and sodium sulfide during Kraft pulping, for example). This leads to
 48 degradation of the non-cellulosic fractions as well as large volumes of effluent
 49 which requires expensive treatment to reduce environmental load.

50 To truly harness the potential of the biorefinery concept, this fractionation step
 51 needs to be revolutionized. It needs to be considerably more process intensive
 52 (ideally seconds per unit volume of biomass -as opposed to minutes or hours) to
 53 enable modular units to deal with large volumes of biomass at decentralized

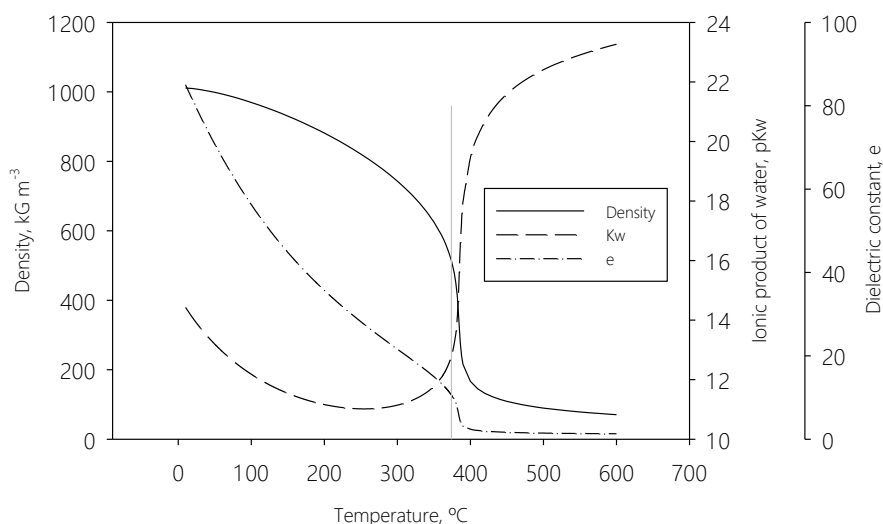
54 locations. It must not involve the use of harsh reagents in order to minimize
55 environmental impact and cost, whilst maintaining quality of the fractions.

56 Water above its critical point (T_c 374°C, 22 MPa), is an alternative solvent for
57 dissolution/hydrolysis of biomass. Its low viscosity and high diffusivity facilitate
58 the penetration of water into the complex structure of the lignocellulosic matrix,
59 whilst its low dielectric constant, similar to non-polar organic solvents, enhances
60 solubility of organic compounds. Physical properties of water (such as density,
61 ionic product, dielectric constant) can be finely tuned by varying temperature and
62 pressure. At these conditions, the hydrolysis of biomass fractions is rapid and
63 presents a mean to achieve significantly more process intensive fractionation of
64 biomass.

65 Reaction speed – whilst being an advantage to process intensification – is also a
66 significant disadvantage to selectivity at longer reaction times, leading to
67 degradation of hydrolysis products and resulting in complex reaction mixtures.
68 This degradation and mixture complexity leads to inefficient recovery of biomass
69 derived products and intermediates. There is therefore a need for understanding
70 the hydrothermal fractionation processes to improve processes selectivity, which
71 can harness the potential of subcritical and supercritical water fractionation.

72 Even under water's critical point, certain fractions of biomass face reactions that
73 proceed too rapidly to be controlled by conventional methods. For instance, lignin
74 undergoes rapid hydrolysis and subsequent hydrolysis product conversion in less
75 than 1 second at 350 °C. Whilst poor selectivity is common to both sub- and
76 supercritical water (SCW), there are some significant differences between the
77 reaction media – most notably the difference in ionic product of water (for
78 example the H^+/OH^- concentration at 300°C and 22 MPa is around $3 \cdot 10^{-6} \text{ mol} \cdot \text{L}^{-1}$
79 vs $3 \cdot 10^{-10}$ at 400 and 22 MPa) which means that subcritical water has a higher
80 concentration of ions ($[H^+]$ and $[OH^-]$) thus favoring ionic reactions vs the radical
81 reactions that are prevalent under SCW conditions.

82



83

84 *Figure 2. Subcritical and supercritical water properties around the critical*
 85 *(22 MPa).*

86 This manuscript studies the lignocellulosic biomass fundamentals fractionation in
 87 subcritical and supercritical water, in order to improve the selectivity of the
 88 hydrothermal biomass fractionation. The manuscript presents four main sections
 89 to presents the fractionation of biomass in hemicellulose, sugars and lignin. As
 90 the biomass structure plays an important role, a section to study the linked
 91 phenols that joint lignin and hemicelluloses is included.

92 2. Hemicellulose(s) fractionation fundamentals

93 Hemicellulose is a biopolymer present in lignocellulosic materials that acts as a
 94 connection between the fibbers (cellulose) and the 3-dimensional structure
 95 (lignin), constituting between 25% and 35% of the whole biomass [1]. It is
 96 characterized by their amorphous structure and by the fact that it is acetylated
 97 [2]. Regarding its composition, it is a biopolymer mainly composed of pentoses
 98 with few hexoses in between, with a maximum length around 200 or 300
 99 monomeric sugars, which makes it a renewable source of chemicals based on 5-
 100 carbon molecules. The maximum molecular weight is lower than 70 kDa in most
 101 cases [3]. However, there are discrepancies between species. For instance,
 102 xylose is the most common monomer in hemicelluloses of hardwood trees, while
 103 softwood trees are principally composed of mannans, like mannose [2]. In
 104 addition, there are two different types of hemicellulose from the extraction

105 viewpoint: one hemicellulose easy to extract and another one that is associated
106 with the fibers of cellulose that can be recovered only when cellulose is also
107 removed (temperatures above 240 °C) [4–6]. Since hemicelluloses have some
108 potentially acidic groups (acetyl groups among others), it can be recovered by
109 Kraft pulping. However, the use of this technique leads to a degradation of
110 hemicellulose, so a different technique is required to obtain it with a high quality.
111 Thus, hydrothermal extraction would be one of the most promising options since
112 it only requires water and mild temperatures (160-210 °C) to extract it [7,8]. If the
113 operational temperature is around 180 °C, 60% of the initial hemicellulose can be
114 recovered as oligomers and sugars [4,9]. Higher yields can be obtained if
115 temperature increases but undesired degradation products appear [10,11].
116 However, hemicellulose can be recovered also at low temperatures (90 °C) if the
117 operating time is high enough (days) [12]. Hemicellulose extraction has been
118 performed in both systems, batch and packed bed reactors. Therefore, it should
119 be also marked that two different operating times can be defined, the solid and
120 liquid time. The former is the time used to treat the solid. The liquid time has the
121 same value as the solid time in batch systems. However, it is fixed by the
122 volumetric flow when semi-batch or continuous system are used, being the
123 residence time (see appendix 1 for more details about the different residence
124 times). Moreover, hemicellulose hydrothermal fractionation is a complex process
125 that involves several physical phenomena [6,8,13,14], which are present as in
126 batch as in continuous systems, and a good knowledge of them is mandatory for
127 designing a profitable and sustainable hemicellulose extraction plant. These
128 phenomena are:

- 129 • Hemicellulose cleaving into decreasing molecular weight oligomers
- 130 • Hemicellulose deacetylation (autohydrolysis)
- 131 • Hemicelluloses dissolution and mass transfer between the solid and the
132 liquid
- 133 • Production of sugars & sugars degradation into furfural or other
134 substances
- 135 • Porosity changes: extraction, swelling and biomass compaction

136 Additionally, and once the phenomenology is explained, a short summary about
137 the effect of the main operational variables on hemicellulose selectivity is
138 included.

139

140 2.1. Hemicellulose cleaving into decreasing molecular weight 141 oligomers

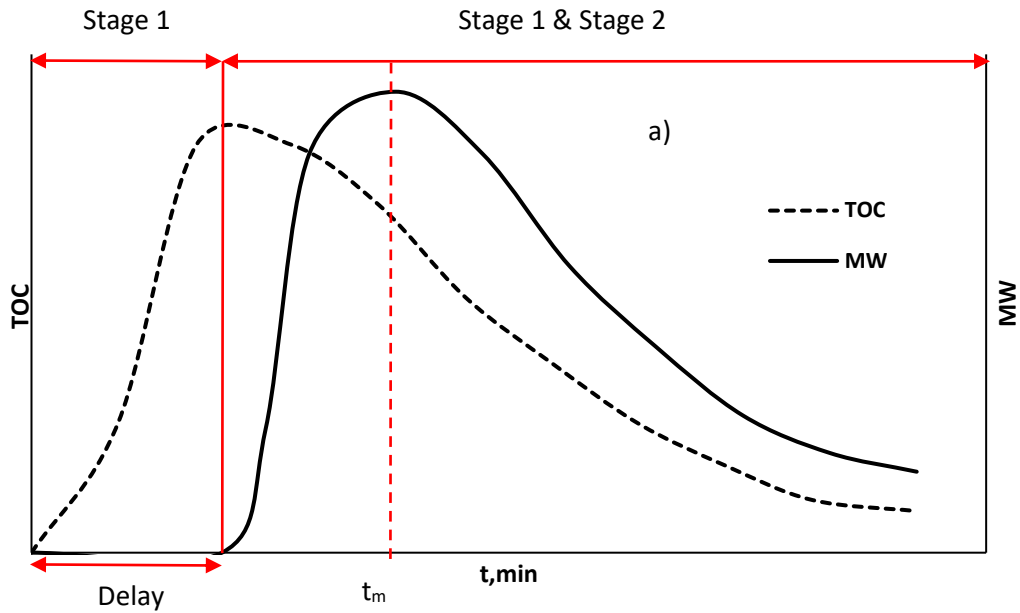
142 The following discussion is focused on the behavior observed in a semi-
143 continuous system since only globalized values can be obtained from a batch
144 reactor. Hemicellulose cleaving is one of the first phenomena that takes place
145 inside a chip or a particle of biomass. Due to the mild operating temperature (e.g.
146 120 to 185 °C), the bonds between the monomeric sugars start breaking
147 randomly, producing progressively shorter oligomers. This process continues
148 until the moment in which the oligomer has a length low enough to be extracted
149 from the solid by solubilization or dragging [6,14,15]. In this moment, both
150 phenomena are present, oligomer dissolution and oligomer cleaving, and two
151 distinct stages can be differentiated: (1) solid oligomer cleaving, which is present
152 from the beginning, and (2) solid & liquid oligomer cleaving with hemicellulose
153 dissolution. The fact that these two phases are present at the same time explain
154 why there is a delay in the extraction profiles (Figure 3.a). Before this first soluble
155 oligomer releasing, only raw material free sugars and a little number of cleaving
156 products (small oligomers and monomers) could be removed. Nevertheless,
157 there are cases where no delay is present due to the biomass diversity [16]. This
158 is possible when the initial hemicellulose length is so low that it is initially soluble
159 or it is so acetylated that only stage 2 is present. Therefore, if both stages are
160 present, the molecular weight evolution during the extraction should have a
161 maximum (the first soluble oligomer) near the time (t_m) when the concentration in
162 the liquid reaches the highest value (Figure 3.b). After this molecular weight peak,
163 it would continuously decrease due to the cleaving. This Behavior was already
164 observed in literature [15,16]. However, when only stage 2 is present the
165 molecular weight would decrease with time.

166

167

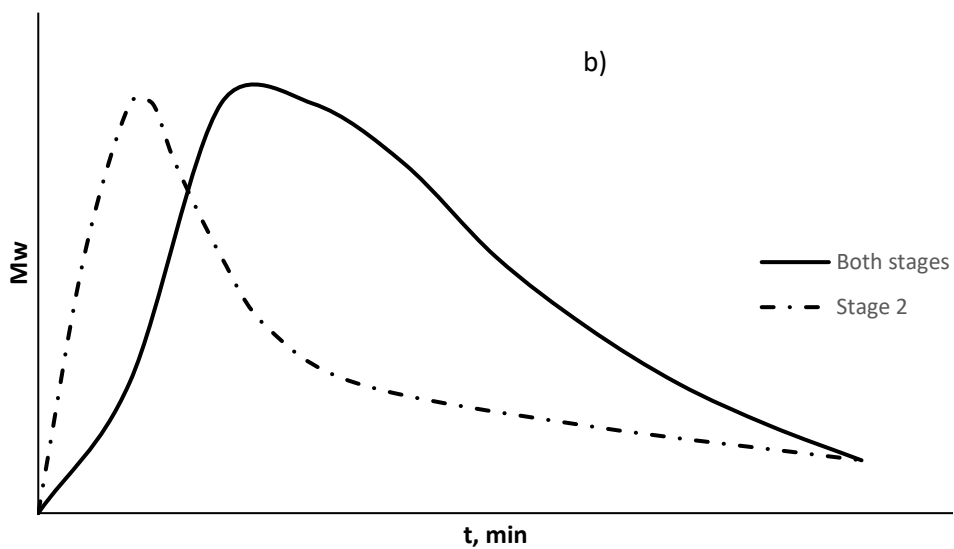
168

169



170

171



172

173

174

175

176

Figure 3: Liquid profiles at the output of a packed bed reactor during a hydrothermal extraction process: (a) TOC evolution, (b) molecular weight evolution (Mw) when both stages are presents and molecular weight evolution when only stage 2 is present.

177

178 To sum up, temperature, the molecular weight and de acetyl contents plays an
179 essential role in hemicellulose extraction since they directly affect hemicellulose
180 solubility.

181 2.2. Sugar production from the cleaving processes

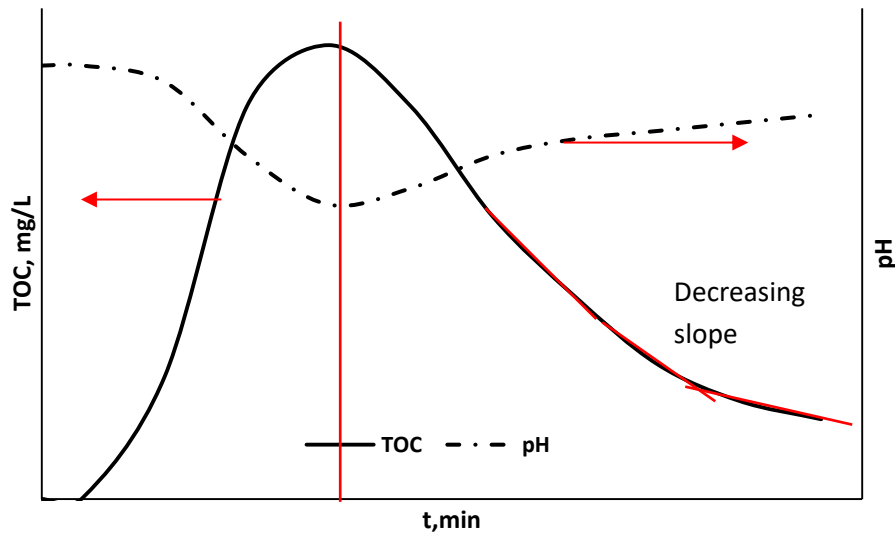
182 As it was explained in the previous section, the cleaving can also produce
183 monomeric sugars and, if temperature is high enough, all the hemicellulose could
184 be converted into monomeric sugars. However, the operational conditions
185 required to achieve a complete conversion are so high that they also imply sugar
186 degradations. *Gallina et al.* [4] studied the optimal conditions for the hydrothermal
187 fractionation of *eucalyptus* in a semi-continuous reactor. They found that the
188 optimum monomeric sugar yield was at 185 °C (67.41%), starting to decrease at
189 higher temperatures. *Yedro et al.* [9] assessed the hemicellulose extraction from
190 *holm oak* in a batch system, obtaining that the highest monomeric yield was at
191 170 °C (60%) and that degradation started at temperatures as low as 150 °C.
192 *Rissanen et al.* [10] analyzed the hydrothermal degradation of spruce in the same
193 reactor as *Yedro et al.* [9], reaching a similar optimum. *Sukhbaatar et al.* [11]
194 worked with sugarcane bagase also in a batch system, being their monomeric
195 yield optimum at 180 °C and observing a huge degradation above 190 °C. The
196 same biomass was considered by *Vallejos et al.* [17] who reached the best
197 monomeric yield at 180 °C too (70%). Similar result were reported by *Thomsen*
198 *et al.*[18], *dos Santos Rocha et al.*[19] and *Makishima et al.* [20] for wheat straw,
199 sugarcane straw and corncob, respectively.

200 Focusing on direct sugar production is of interest since they can be used to
201 produce fuels (bioethanol) or chemicals (like xylitol via hydrogenation). These so-
202 called “degradation products” can also be the target [8]. For instance, furfural and
203 its derivatives can be used as fungicides or lubricants [21] while lactic acid is a
204 precursor for biodegradable polymers production [22]. Therefore, to
205 avoid/promote sugar degradation the operating temperature and the volumetric
206 flow (the less time in the reactor, the lower degradation [4,7,18,20] are the main

207 involved variables. It is worth highlighting that when the reactor is a batch system,
208 the liquid/solid ratio has the same role as residence time.

209 2.3. Hemicellulose deacetylation

210 Hemicellulose deacetylation and cleaving take place in parallel, which is reflected
211 in a releasing of acetic acid during the hemicellulose extraction, decreasing the
212 pH of the water. It should be remarked that this acetic acid production only
213 happens in the solid phase [6,14,23–25]. However, acetic acid can be obtained
214 from sugar degradation in liquid phase too [8]. Similarly, uronic acid can be also
215 released during the hydrothermal treatment [26,27]. Nevertheless, it is not
216 completely clear if the pH change accelerates extraction or if this change is only
217 a consequence of the extraction [10,12]. This phenomenon is deeply related with
218 the hemicellulose extraction process selectivity since these acids are a source of
219 protons that catalyze the cleaving and degradation reactions in liquid phase if the
220 residence time is high enough [6,14]. A statement that was verified by *Song et al.*
221 [28], showing that degradation is much lower if the pH is maintained above 4-5.
222 Moreover, the releasing of acetyl groups also means that the solubility of the
223 remained part of the hemicellulose would be lower since the capacity of linking
224 by hydrogen bonds with water would be lower. Additionally, the steric hindrance
225 also would be higher. Following this idea, it can be seen in Figure 4. that the
226 minimum of the pH corresponds to the maximum in the TOC profile. Thus, the
227 oligomers involved in the stage (2) defined in Figure 3 will be more soluble since
228 they are smaller but, at the same time, their solubility also decreases due to the
229 lack of acetyl groups, explaining why the extraction is more difficult after the
230 maximum (decreasing slope). Moreover, extraction would also be slower
231 because the available amount of hemicellulose is much lower. Thereby, the
232 acetylation degree (and uronic content) is another variable to consider.



233

234 *Figure 4: Relation between the pH and the extracted biomass.*

235 2.4. Hemicellulose dissolution and mass transfer

236 Hemicellulose solubility has been already discussed in section 2.1. External and
 237 internal mass transfer resistances can be present in this process. External mass
 238 transfer can be enhanced by a proper mixing for batch extraction in a stirred
 239 vessel or by high volumetric flows for semi-continuous and continuous extraction
 240 in tubular beds. Furthermore, internal diffusion problems can be minimized if the
 241 particle diameter is low enough. *Rissanen et al.* [10] indicated that the size of the
 242 extracted hemicelluloses is highly dependent on the initial particle diameter.
 243 When using particle size below 2-3 mm hemicelluloses are relatively easily
 244 extracted from the matrix and higher molecular weights are obtained. By contrast,
 245 when a bigger particle size is used, e.g. 1 cm chips, water comes inside the chip
 246 and the hydrolysis starts to take place. If deacetylation occurs, which is probable,
 247 then the acetic acid lowers the pH inside the chip accelerating the cleavage.
 248 Depending on the internal and external mass transfer of the protons, the time with
 249 low pH inside particle will be different and the final molecular weight will be also
 250 affected. In general, the smaller the particle sizes, the higher the molecular
 251 weights. However, it has been widely demonstrated that temperature and solid
 252 operating time have a bigger impact on the yield, promoting extraction when they
 253 are increased [4,7,9–13,15–20,29].

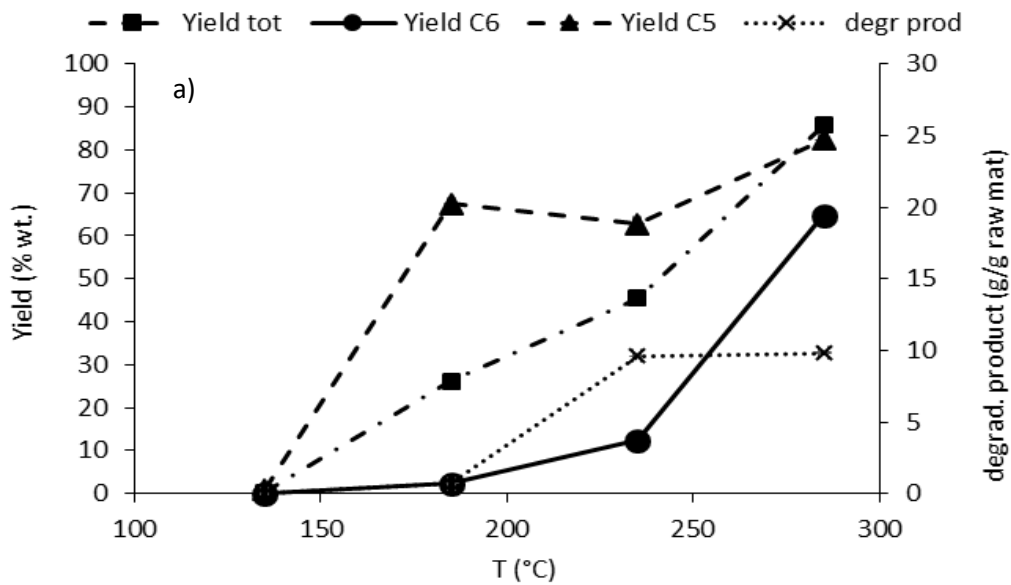
254 2.5. Porosity changes: extraction, swelling and bed 255 compaction

256 During extraction, it is expected that the porosity of the bed increases since a
257 certain amount of mass is being removed. However, if this extraction was
258 important enough, the bed could collapse, reducing the porosity and making it
259 impossible to continue the extraction (tremendous pressures drops). Additionally,
260 biomass also can swell [6,13,14]. Therefore, a preliminary study about the
261 behavior of the packed during the extraction should be required to avoid
262 operational problems.

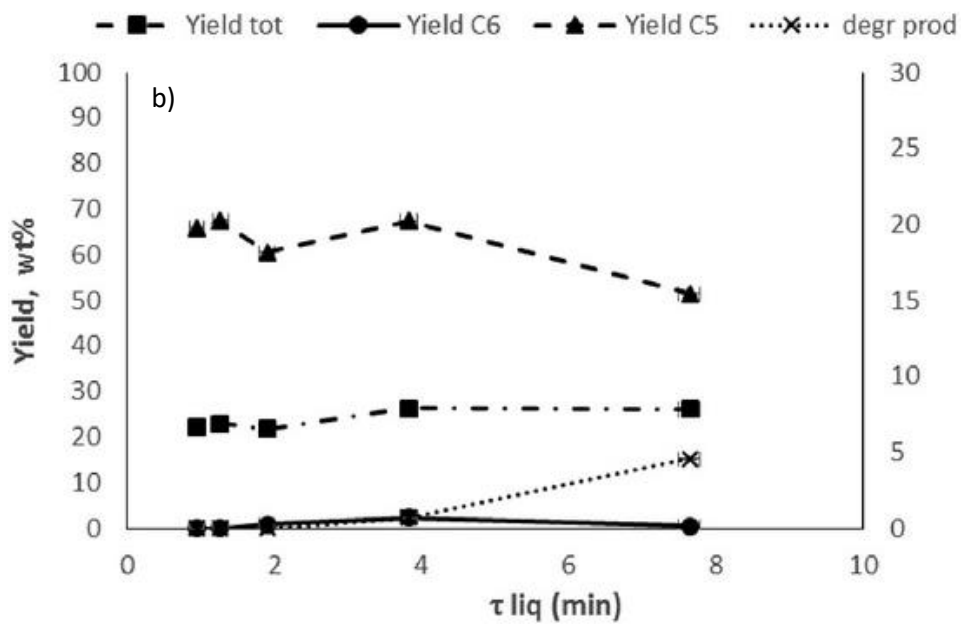
263 2.6. Main variables on extraction selectivity: oligomers and 264 monomers as target compounds

265 It can be concluded from the discussion done from sub-section 2.1 to 2.5 that the
266 main variables to promote hemicellulose extraction yield are the solid operational
267 time and the operating temperature. Therefore, the higher the temperature/time
268 is, the bigger yield is obtained. However, if these two variables are too high,
269 hemicellulose sugars and oligomers start to degrade, reducing the selectivity
270 [4,30]. For instance, this temperature effect can be easily seen in **Figure 5.a**,
271 where it can be checked that at temperatures higher than 180 °C the yield of
272 pentoses (C5) decreases although the global yield increases (Yield tot).
273 Additionally, it is also worth mentioning that if temperature goes above 240 °C,
274 cellulose extraction would take place making it possible to recover the
275 hemicellulose **fraction associated with cellulose** and explaining the increase in
276 the yield. Nevertheless, this higher temperature would also mean the releasing
277 of hexoses and cellulose oligomers and the extraction of some lignin fractions
278 [6,31,32], which would reduce the hemicellulose selectivity. On the other hand,
279 not only does the solid time and the temperature control selectivity, but also the
280 liquid residence time and the operational pH affect it. If residence time is low
281 enough, sugar degradation can be avoided (**Figure 5.b**). Regarding pH, it has
282 been demonstrated that degradation can be reduced up to around 90% if pH is
283 maintaining upper than 4-5 [33]. To sum up and provided that a high

284 hemicellulose selectivity is desired, temperatures around 180 °C, pH above 4 and
 285 high volumetric flows (residence time lower than 4 min) are required.



286



287

288 *Figure 5: Hydrothermal extraction of eucalyptus in a semi-continuous reactor*
 289 *(solid time of 90 min): evolution of the hemicellulose extraction yield (Yield tot),*
 290 *the yield of hexoses (C6), pentoses (C5) and degradation products for*
 291 *eucalyptus with temperature (a) and residence time at 185 °C (b) [4]*

292

293

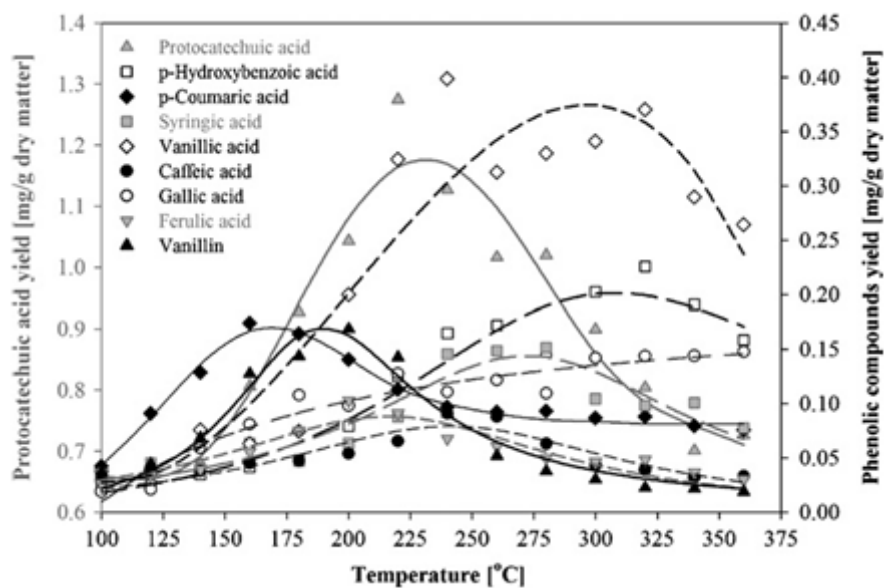
294 3. Bound phenolics

295 Phenolic compounds are of great interest due to their antioxidant properties and
296 potential health benefits that make them useful in numerous commercial
297 applications in the food, cosmetic and pharmaceutical industries [34]. They can
298 be present in the matrix in three forms: free, soluble-bound (esterified to low
299 molecular mass compounds) or in an insoluble-bound form (esterified and/or
300 etherified to cell wall structural components) [35]. **In cereal brans and in some
301 whole cereals, they are found approximately in the proportion 0.1:1:100, so at the
302 beginning the free and soluble-bound moieties are negligible, but after applying the
303 treatment that release the bound moiety from the solid, both soluble forms are of
304 great importance. Moreover, the free and soluble-bound moieties present initially
305 in the solid** are removed with the extractives and in this section the release of the
306 bound moiety is analyzed.

307 Phenolic acids are a subgroup of phenolic compounds of great importance in
308 cereal grains, which are mostly found in the insoluble form. Among them, ferulic
309 and coumaric acid (two hydroxycinnamic acids) are the most studied ones due to
310 its abundance in the plant kingdom. They provide rigidity to the cell wall [36] as
311 they crosslink the sugar moieties and also the lignin. Despite being minor
312 compounds (around **0.5-1%** in cereal brans) their high value can enhance the
313 profitability of the biorefinery and in order to recover them, it is necessary to
314 hydrolyze the ester and/or ether bonds that maintain them attached.

315 Alkaline hydrolysis is the most common procedure used for their releasing [37]
316 but it is a non-selective method that also alter the whole matrix. On the other
317 hand, enzymatic hydrolysis can be selective if the proper enzymes are chosen,
318 but it must be taken into account the matrix as well as the main phenolics present
319 [38]. Feruloyl esterases (EC 3.1.1.73) are a family of enzymes able to cleavage
320 the ester bond between the hydroxycinnamic acids and the sugar moieties, but in
321 some cases where the yield is low, the use a mixture of enzymes including
322 xylanases lead to increase it significantly [39]. In this context, the use of
323 pressurized water emerge as an interesting technique, which shorten
324 considerably the extraction time and avoid the use of solvents and/or expensive
325 enzymes. The optimum temperature, pressure and extraction time vary

326 depending on the raw material used and the main phenolic present. As the major
 327 part of them are etherified to hemicelluloses and the ether bonds are labile at
 328 170°C [35], temperatures higher than that are commonly used and as
 329 consequence, the co-extraction of the hemicellulose also takes place. After a
 330 certain temperature, or long extraction times, the phenolic compounds start to
 331 decompose due to their thermal degradation. The effects named above can be
 332 seen in Figure 6 where *Pourali et al.* [40] studied the effect of temperature on the
 333 extraction yield of different phenolic acids from defatted rice bran, and obtained
 334 different optimum temperatures for each phenolic acid. In the first stage, the ether
 335 links are being released and the co-extraction of the hemicellulose enhance the
 336 extraction, favoring the solvent penetration and the mass transfer; in the second
 337 stage, the degradation of the phenolic compounds turn out to be higher than the
 338 release, and so on, the extraction yield decrease.



339

340

341 *Figure 6. Effect of subcritical water temperature on the extraction of different*
 342 *phenolic compounds from defatted rice bran (residence time = 10 min).*

343

Obtained from Pourali et al [40]

344

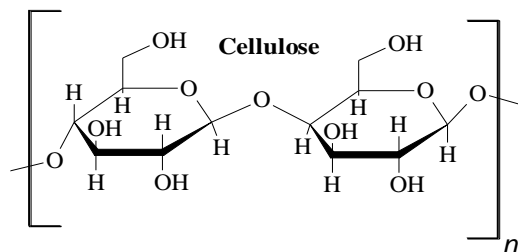
345 Therefore, after selecting the optimum conditions to maximize the extraction of
 346 the target compound(s), a purification step is necessary to separate the phenolic
 347 fraction from the hemicellulose fraction. However, this optimum condition should

348 be chosen avoiding or reducing the alteration of the cellulose and lignin fractions,
349 as in the biorefinery process they will be separated in a next step.

350

351 4. Cellulose

352 Cellulose is a renewable, cheap and worldwide-distributed polymer with very
353 promising applications for the future industries. Cellulose is a linear-chain
354 polysaccharide consisting on units of glucose linked by β -1,4 glucosidic bonds,
355 which structure is shown in Figure 7. Its formula is $(C_6H_{10}O_5)_n$, where n is the
356 degree of polymerization and goes from several hundred to many thousands of
357 glucose units, depending on the raw material. The hydrogen bond network
358 between OH groups in its structure promotes the aggregation of cellulose chains
359 forming fibrils [41]. These fibrils are tough, water insoluble and forms the
360 foundations of the plant cell walls [42–44]. For mass production, cellulose is
361 obtained from plants, bacteria, algae and fungi via biosynthesis or in-vitro
362 synthesis [45]. Although synthesized cellulose has numerous applications and
363 uses, it is not the only way to make profit out of residual biomass.



364

365

Figure 7. Cellulose formula

366 Lignocellulosic biomass is a complicated matrix formed by an intricate network
367 where cellulose, hemicellulose and lignin are linked and interacting together.
368 Conversion of these biomass fractions into valuable products is the key step for
369 the success of the bio-based future industries, where agricultural or industrial
370 wastes usually regarded as worthless would be converted into chemicals, fuels
371 and/or energy. In order to get these valuable products from lignocellulosic
372 biomass, depolymerization and hydrolysis of cellulose to monomer glucose is
373 regarded as a necessary first step [46]. Hydrolysis reaction implies the cleavage
374 of a chemical bond by the addition of water [47]. However, as mentioned above,

375 cellulose is a water insoluble polymer so that it is not possible to simply dissolve
376 and hydrolyze cellulose in water at ambient conditions. As a result, the hydrolysis
377 of cellulose in lignocellulosic biomass usually involves the use of strong acids as
378 catalysts [46], which cause a negative impact in the environment and yields a
379 high concentration of degradation products. However, when using supercritical
380 water cellulose is more effectively converted to oligomers and monomer sugars
381 instead of yielding mainly degradation products.

382 Therefore, the objective of this section is to clarify the mechanisms involved in
383 both the dissolution and the hydrolysis of cellulose in water as well as to discuss
384 the influence of the key parameters which affect both processes.

385 4.1. Cellulose dissolution

386 The dissolution of cellulose in water have been explained [48–50] from a
387 thermodynamic point of view. The Gibbs free energy is a thermodynamic
388 magnitude commonly considered to analyze whether a chemical process is
389 spontaneous or not. Its variation is expressed as a combination of the variation
390 of the enthalpy and the variation of the entropy of the system:

$$391 \Delta G = \Delta H - T\Delta S \quad (1)$$

392 “G” is the Gibbs free energy, “H” the enthalpy, “T” the temperature and “S” the
393 entropy. When the variation of the Gibbs free energy is negative, the process is
394 spontaneous. In the reaction of two different compounds, the variation of enthalpy
395 represents the heat of reaction or the heat of mixing. In the combination of
396 cellulose and water this parameter is almost negligible since no additional heat is
397 generated or consumed. Therefore, the previous expression is reduced to:

398

$$399 \Delta G = -T\Delta S \quad (2)$$

400

401 Consequently, the dissolution and hydrolysis of cellulose in water is carried out
402 (spontaneous process) when the entropy variation is positive. From a structural
403 point of view, the entropy of cellulose increases when its molecular conformation
404 changes from a rigid structure to a more flexible one which benefits dissolution.
405 Since cellulose structure is characterize by its complexity and rigidity, at lower

406 temperatures no conformational changes will be produced, the entropy will not
407 increase nor the Gibbs free energy will decrease and therefore no dissolution will
408 be produced. Only in the cases in which the temperature is considerably
409 increased and therefore the internal energy of the structure, conformational
410 changes could be produced.

411 In literature, three main characteristics of the cellulose structure are considered
412 of fundamental interest in its dissolution in water:

413

414 1) The presence of intra and intermolecular hydrogen bonds [48,49,51].
415 Cellulose is constituted by glucose molecules joined together forming long
416 fibbers which are connected by hydrogen bonds. This fact results in a rigid
417 and cohesive structure which avoids the penetration of water molecules and
418 consequently the dissolution of the structure.

419 2) Cellulose is considered an amphiphilic molecule [48,49,52]. Its structure has
420 both hydrophobic and hydrophilic zones as a consequence of the orientation
421 of its functional groups. While the hydroxyl groups located in equatorial
422 position create the hydrophilic regions, the axial glycosidic bonds produce
423 hydrophobicity. This is considered the reason why the water molecules are
424 not able to easily create hydrogen bonds with the cellulose which will
425 produce its dissolution.

426 3) Crystallinity: crystallinity has always been considered a key parameter when
427 analyzing the dissolution of cellulose in water [48,53]. The high crystallinity
428 of the cellulose molecule is responsible of its rigid structure avoiding
429 conformational changes which could facilitate its dissolution.

430 Considering the lack of a robust model which explains the dissolution of cellulose
431 in water, several authors have performed experiments with the objective of
432 analyzing the influence of the process parameters.

433 From a structural point of view, [54,55] studied the influence of the raw cellulose
434 used in the dissolution. They demonstrated that the cellulose allomorph directly
435 affects the dissolution process. For example, although cellulose I is the most
436 abundant type in nature, cellulose II is more stable [49]. Moreover, not only the
437 cellulose type influences the dissolution, also the amount of water has to be
438 considered [48,56]. Regarding to the crystallinity of the structure, [57] analyzed

439 the dissolution of cellulose after milling. Milling produces an amorphous structure
440 which facilitates the action of water. They stated that the critical factor is not the
441 reduction of the particle diameter but the cleavage of the hydrogen bonds and
442 the consequent generation of amorphous zones. Amorphous and semi-crystalline
443 zones are easier to be hydrolyzed since water molecules can avoid the
444 hydrophobic zones which are present in the structure as a consequence of the
445 amphiphilic nature of the cellulose [58].

446 From an operating point of view, the majority of experiments analyzed the
447 process focusing in the variation of the pressure, the temperature and the
448 reaction time. As it has been explained in this section, due to the physical
449 structure and the nature of cellulose, its dissolution is greatly limited by
450 temperature. Common working temperatures usually range from 200°C to more
451 than 400°C. Therefore, in order to maintain water in liquid or supercritical state
452 when the working conditions surpasses its critical point, ($T_c=374^\circ\text{C}$, $P_c=22.1$
453 MPa) the pressure shall be increased. The analysis of the influence of pressure
454 has been studied by [53]. They proved that when the pressure is increased above
455 50MPa (reaching pressures up to 700MPa), even at relative low temperatures
456 the water molecules are able to enter inside the cellulose structure and swell the
457 polymeric matrix which finally collapses. When the pressure is only considered in
458 order to maintain the water in liquid or supercritical state, its influence is negligible
459 and the fundamental parameters to be considered are the temperature and the
460 reaction time. An increase of temperature clearly benefits the dissolution of
461 cellulose since it modifies its structure favoring the combination of cellulose and
462 water molecules. However, it also accelerates its hydrolysis consuming the
463 cellulose which is being dissolved. Consequently, the only possibility of dissolving
464 cellulose and reduce its hydrolysis rate is selecting an optimum combination of
465 temperature and reaction time. In literature, the analysis of cellulose dissolution
466 at high temperatures is generally combined with hydrolysis studies. Hydrolysis is
467 considered one of the fundamental processes in green chemistry since it allows
468 obtaining high value products from renewable resources such as biomass. As
469 biomass is a complex raw material and due to the lack of enough know-how in
470 this field, the majority of authors have started working with cellulose instead of
471 with biomass. When cellulose is mixed with water at high temperatures, it is first

472 dissolved and subsequently it reacts with the water molecules present in the liquid
473 medium producing the cleavage (hydrolysis) of the glycosidic bonds. As the
474 cleavage of these bonds is not completely simultaneous nor instantaneous, first,
475 oligosaccharides are generated which are then hydrolyzed to monosaccharides.
476 Finally, if the hydrolysis reaction is not stopped, the monosaccharides are
477 degraded to organic compounds such as acids [59,60]. As it has been stated, it
478 is fundamental both in dissolution and in hydrolysis to find the optimum pair of
479 temperature and reaction time values in order to reduce the generation of
480 undesired products.

481 The experiments presented in literature are clearly divided in three zones:
482 subcritical region, vicinities of the critical point and supercritical region.

483 In this paper, the subcritical region is considered the one in which the temperature
484 remains below 320°C. In this zone the dissolution and subsequent hydrolysis is
485 produced as a result of the consumption of superficial cellulose which is able to
486 interact with water molecules [61]. Furthermore, the cellulose which can be easily
487 dissolved is the one which was present in an amorphous state. Below 280°C, it
488 is observed that the cellulose dissolution rate decreases with time since water is
489 not able to dissolve crystalline cellulose once the amorphous cellulose has been
490 already dissolved [55]. At temperatures between 280°C and 320°C increasing
491 either the reaction time or the temperature only increases the degradation of the
492 cellulose, mostly amorphous, which has been already dissolved [55,62].
493 Therefore, working with low reaction times produces high DP (degree of
494 polymerization) molecules [63]. At temperatures below 250°C [64] proved that
495 cellulose is dissolved but not hydrolyzed and therefore that it is possible to obtain
496 high DP molecules. However, the process is limited by the amount of amorphous
497 cellulose available. In these cases reaction times in the order of hours are
498 required which implies the operation in batch and semi-continuous reactors.
499 Finally, milling the raw cellulose creates amorphous zones which can be easily
500 dissolved, even at temperatures below 230°C, generating high DP molecules
501 [57]. At this temperatures, no modifications are observed in the solid residue
502 when the cellulose structure is crystalline instead of amorphous [65].

503 In the region near the critical point, when the reaction time is increased, the
504 dissolved cellulose is hydrolyzed to glucose and lately to degradation products.

505 It has been experimentally demonstrated [51] that at temperatures between
506 320°C and 330°C (25MPa) a transition from a crystalline to an amorphous
507 structure is produced. This transition explains the rapid dissolution of cellulose in
508 water and the absence of any swelling phenomena [51]. The fact that when
509 cellulose and water react at these or higher temperatures during a short reaction
510 time the final product obtained is cellulose II when the initial cellulose allomorph
511 is cellulose I is justified as a consequence of the higher stability of cellulose II.
512 When the temperature is increased above 330°C cellulose I is converted into
513 amorphous cellulose. Then, when the temperature decreases, the amorphous
514 cellulose is converted into the more stable cellulose II allomorph [59,61]. This is
515 also confirmed working at temperatures below 320°C since only cellulose I is
516 obtained [66].

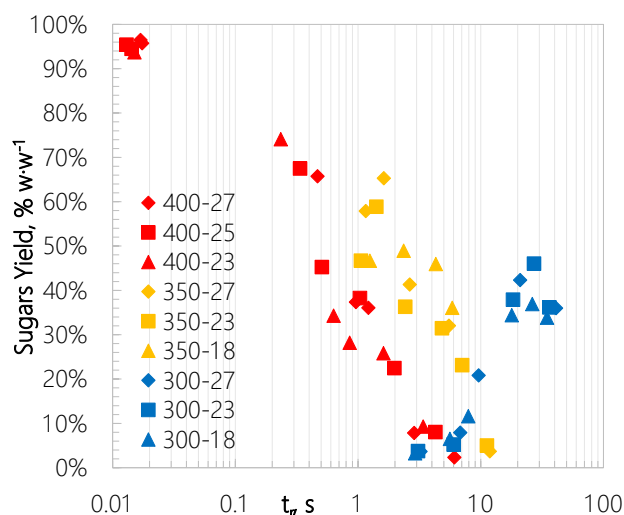
517 Finally, in the supercritical region the dissolution and hydrolysis of cellulose when
518 working at low concentrations is produced simultaneously, in homogeneous
519 phase and without mass transfer limitations [53,67]. The transition between
520 crystalline cellulose to amorphous cellulose at 330°C, the high temperatures of
521 reaction which produce the cleavage of the hydrogen bonds [53,68] and the
522 properties of supercritical water such as high diffusivity, high density compared
523 with water in vapor state and its ability to dissolve organic compounds, observing
524 the total dissolution of cellulose [69,70], explain the homogeneity of the process.
525 Recently it has been proved that when the concentration of cellulose is increased
526 the dissolution and hydrolysis processes are not completely simultaneous nor
527 homogeneous [71].

528 4.2. Cellulose hydrolysis

529 It is noted that in this reaction zone the hydrolysis of biomass has gained a lot of
530 attention [67,68]. In fact, special attention has been paid to the hydrolysis of
531 cellulose, since it is the major component of lignocellulosic biomass and therefore
532 is the key to better understand the reaction mechanisms, kinetics and
533 performance of supercritical water hydrolysis of real biomass [71,72].

534 4.2.1. Production of sugars from cellulose hydrolysis in supercritical 535 water

536 The conversion of cellulose to sugars in supercritical water has been extensively
537 studied using different kinds of reactors. The hydrolysis in batch-type reactors is
538 usually carried out with long reaction times, favoring the decomposition of glucose
539 to degradation products [73,74]. However, the flow-type system makes it possible
540 to reduce the reaction time and therefore increasing the yields of sugars instead
541 of degradation products [61,70]. Recently our research group developed an
542 experimental set up to perform the hydrolysis of cellulose suspensions in
543 supercritical water by using a continuous micro-reactor, giving as a result a total
544 conversion of cellulose in milliseconds and yielding a sugars production of 96 %
545 w/w [67]. This continuous micro-reactor is shown in Figure S2, where it can be
546 seen that the reaction section consisted of a tee junction (M) where the cellulose
547 (or biomass) was instantaneously heated up by mixing it with a supercritical water
548 stream. In order to effectively stop the hydrolysis reaction, a sudden
549 depressurization through a needle valve was carried out, so that the effluent was
550 immediately cooled down from 400°C to around 100°C and therefore reaction
551 was over. Then, depending on the dimensions of the pipe between the junction
552 and the depressurization valve, the reaction time was calculated as a function of
553 reactor volume and flow to the reactor, so that just by changing the dimensions
554 of the reactor of the pumped flow, different reaction times would be provided. In
555 terms of sugars yield from cellulose hydrolysis in hydrothermal medium, several
556 conditions were tested by changing temperature, pressure and reaction time in
557 the micro-reactor mentioned above. As a result, it was found that the optimal
558 conditions to obtain soluble sugars (up to six units of glucose) were achieved at
559 400 °C with extremely short reaction times (around 0.01 s). If the reaction time
560 was increased, the sugars were hydrolyzed and the yield decreased, as it can be
561 seen in Figure 8. The combination of supercritical water medium and the effective
562 method for the reaction time control allowed such a high sugars yield from
563 cellulose hydrolysis. This fact can be explained taking into account than under
564 those conditions, the cellulose hydrolysis kinetics are improved and the glucose
565 hydrolysis kinetics are slow enough so that using the sudden expansion micro-
566 reactor is possible to stop the reactions after complete cellulose hydrolysis but
567 before glucose degradation [67]. It was also proven that cellulose hydrolysis
568 reactions were highly influenced by temperature, meanwhile pressure did not
569 affected cellulose hydrolysis rate in the studied range [75,76].



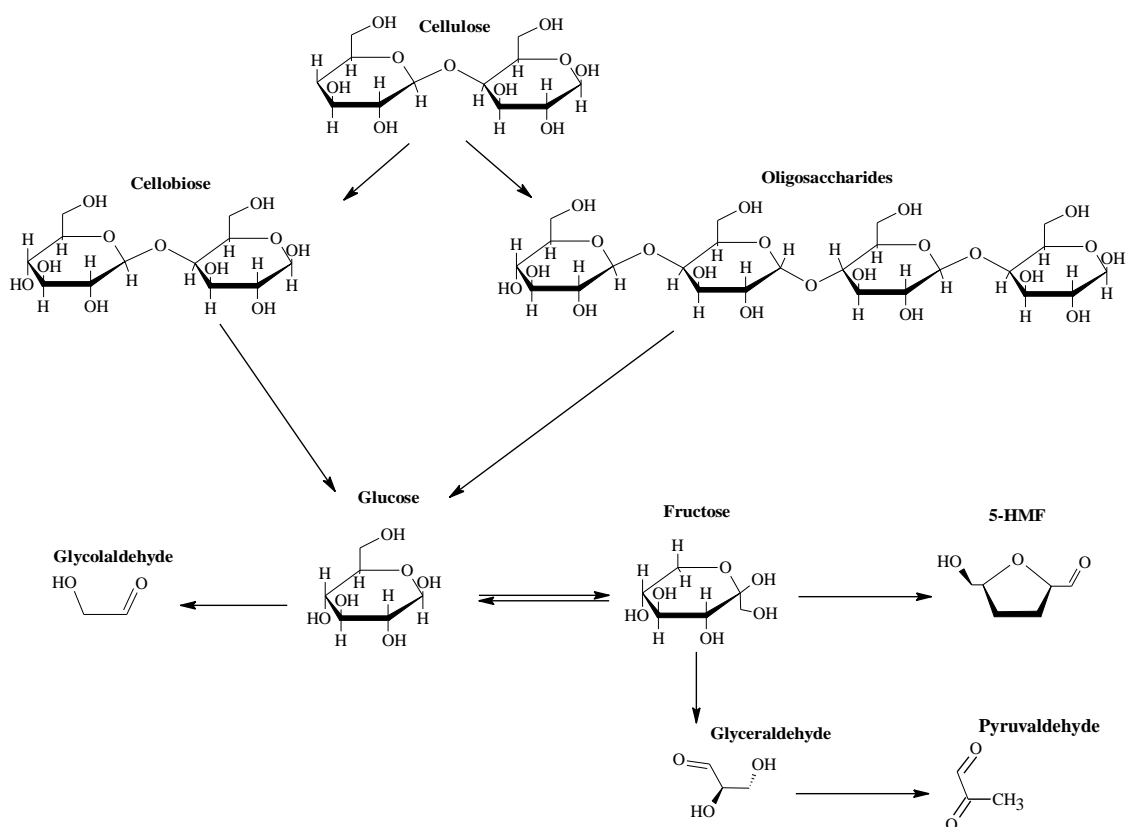
570

571 *Figure 8. Sugars yield from cellulose hydrolysis in hydrothermal medium along*
 572 *reaction time. Experiment temperature: red = 400°C; yellow = 350 °C; blue =*
 573 *300°C. Experiment pressure (◆) 27 MPa; (■) 25 / 23 MPa and (▲) 23 / 18 MPa*
 574 *[76].*

575

576 4.2.2. Cellulose hydrolysis kinetics in supercritical water

577 Cellulose was hydrolyzed following the main hydrolysis reaction pathway in
 578 supercritical water which is shown in Figure 9 [71], where it can be seen that
 579 cellulose is firstly hydrolyzed into oligosaccharides and then into glucose. Once
 580 the glucose has been produced, it can be isomerized to fructose and then
 581 converted into dehydrated (5-HMF) or retro-aldol condensation products
 582 (glycolaldehyde, pyruvaldehyde and/or glyceraldehyde). As mentioned above,
 583 working at 400 °C and very short reaction times, the reaction would be stopped
 584 at glucose. However, if the reaction time is increased, retro-aldol condensation
 585 products would be produced, yielding aldehydes as glycolaldehyde,
 586 pyruvaldehyde and/or glyceraldehyde. Therefore, the control of reaction time was
 587 the key factor to selectively hydrolyze cellulose in supercritical water.

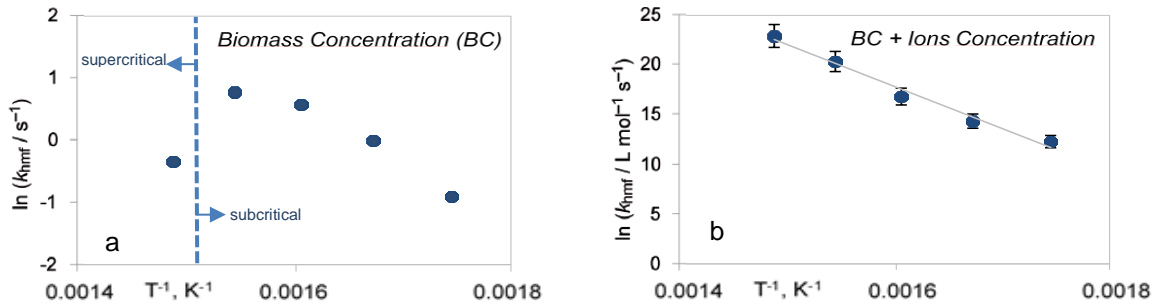


588

589 *Figure 9. Reaction pathway for cellulose hydrolysis in supercritical water based*
 590 *on [71].*

591 The properties of water may vary considerably when changing the conditions
 592 from subcritical to supercritical, affecting to the products yielded from cellulose
 593 hydrolysis [72]. Just by changing pressure and temperature, different reaction
 594 mechanisms are favored. Water at 25MPa and temperatures below 300 °C has
 595 a density around 800 kg/m³ and an ionic product (as *pK*) between 11 and 14.
 596 Under those conditions, water is highly dissociated and H⁺/OH⁻ ions are highly
 597 available in the reaction medium and therefore ionic reactions are favored [77,78].
 598 However, when temperature is increased up to 400 °C at constant pressure, the
 599 density considerably decreases (being around 150 kg/m³) and the ionic product
 600 increases up to 21 [79]. This change in the ionic product affects the kinetics of
 601 glucose and fructose degradation, avoiding the ionic degradation reactions
 602 (which are the governing chemistry when using acid catalysts) and favoring the
 603 radical reactions [72]. In fact, it was found that the concentration of H⁺/OH⁻ due
 604 to water dissociation was a determining factor in the selectivity of cellulose
 605 hydrolysis in supercritical water [76]. So far, kinetic models for cellulose
 606 hydrolysis only considered the concentration of cellulose and its derived products

607 into the equations, so that first order kinetics were selected to predict cellulose
608 hydrolysis in supercritical water. Following those traditional kinetic models
609 Cantero *et al.* [76] found an incongruity for the kinetic constants of fructose
610 dehydration to 5-HMF when carrying out the hydrolysis of cellulose in supercritical
611 water at temperatures between 300 – 400 °C and 25 MPa. In Figure 10 it can be
612 seen the fitted kinetic constants of 5-HMF formation (k_{hmf}) versus the reciprocal
613 temperature, according to Arrhenius law. A break point can be clearly observed
614 in Figure 10a, corresponding to the surroundings of the critical point of water,
615 which represents a deviation from Arrhenius law. So that, the traditional models
616 where only cellulose concentration was taken into account in a first order kinetics
617 equation were only capable to predict the kinetic constants of fructose
618 dehydration to 5-HMF at subcritical conditions. That suggested that another
619 factor was not taken into account into the kinetic equation. To solve the problem,
620 the concentration of protons and hydroxide ions were added to the kinetic model,
621 turning it into a second order kinetic equation. As a consequence of that
622 transformation, the kinetic constants followed the Arrhenius law for the full
623 temperature spectra, meaning that the dehydration to 5-HMF under both
624 subcritical and supercritical conditions was lineally fitted as it can be observed in
625 Figure 10b. That would suggest that the selectivity of the process was strongly
626 affected by the protons and hydroxide ions concentration in the reaction medium,
627 so that improving the understanding of the reaction mechanisms of the hydrolysis
628 of cellulose in supercritical water. In that way, retroaldol condensation reactions
629 from glucose and fructose (to produce aldehydes) are not very demanding of ions
630 and therefore they are favored when water is highly associated (as it occurs at
631 supercritical state). On the other hand, isomerization glucose-fructose and
632 dehydration reactions are not favored since these reactions take place forming
633 transition states with OH^- and H^+ and thus they are diminished when water is
634 highly dissociated [76].



635

636

637 *Figure 10. Kinetic constants Arrhenius fitting for fructose dehydration to 5-HMF*
 638 *at 25 MPa and temperatures between 300 and 400°C [76]. a) Kinetic evaluation*
 639 *just considering cellulose and derived products concentration. b) Kinetic*
 640 *evaluation also considering protons and hydroxide ions concentrations as*
 641 *reagents.*

642

4.2.3. Cellulose concentrations as a mass transfer limitation

643

644

645

646

647

648

649

650

651

652

653

654

655

656

657

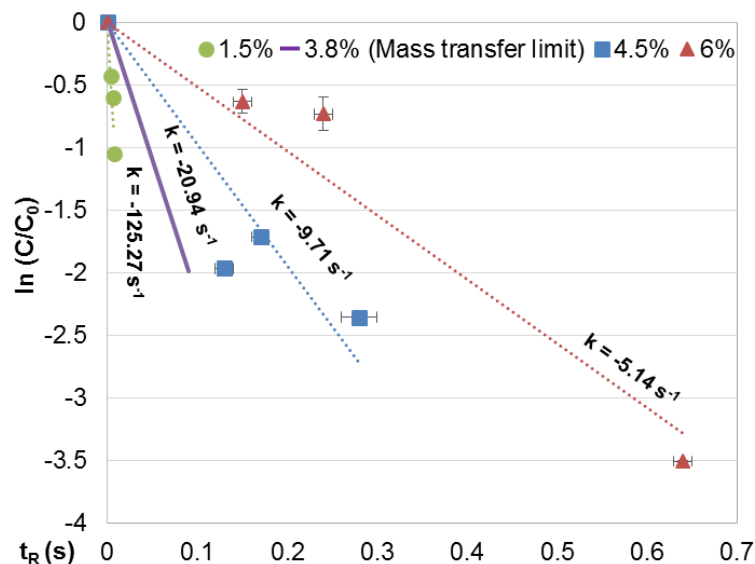
658

659

660

Another factor recently revised concerning cellulose hydrolysis and dissolution in supercritical water was the effect of cellulose concentration itself [71]. So far, existing models describing the conversion rate of cellulose assumed that the hydrolysis of cellulose particles takes place at their surface and therefore the particle size was considered the key parameter for the conversion rate. That shrinking-core model implied the use of a nonconventional kinetic equation [66,72]. On the other hand, to take into account the reagent concentration, a first order kinetic was assumed to describe the conversion rate of cellulose in supercritical water. As it can be seen in Figure 11, experimental results of cellulose hydrolysis in supercritical water at 400 °C and 25 MPa and different concentrations were fitted to the first order kinetic equation by plotting the logarithm against the reaction time. In all cases, a linear dependence was found, where the slope represented the kinetic constant, k . In Figure 11 it can be observed that when increasing the cellulose inlet concentration the reaction rate is slower, suggesting that mass transfer resistances must have an important effect over cellulose hydrolysis kinetics. Also, combining those data with the ones from a previous work [67] it was possible to calculate the so called *mass transfer limit* for cellulose hydrolysis in hydrothermal media. Those calculations are

661 detailed in another work from our research group [71]. It was mathematically
 662 possible to distinguish between homogeneous and heterogeneous reaction
 663 medium, just by calculating a new kinetic constant (-20.94 s^{-1}), which
 664 corresponded to an inlet concentration of 3.83 % w/w (identified as *mass transfer*
 665 *limit*). When the concentration was lower than the *mass transfer limit*, cellulose
 666 was completely solubilized in supercritical water and it can be considered that the
 667 hydrolysis occurred in a homogeneous phase and thus the conversion rate was
 668 higher. On the contrary, if the concentration was higher than 3.83 %, the cellulose
 669 behaved as if it was hydrolyzed at subcritical conditions. For this subcritical
 670 hydrolysis-like, the cellulose was not totally dissolved and hydrolysis reaction
 671 occurred in a heterogeneous phase.



672
 673 *Figure 11. Kinetic analysis for cellulose concentrations of 5, 15 and 20 % w/w*
 674 *(corresponding to 1.5, 4.5 and 6 % w/w at the reactor inlet). The regression*
 675 *coefficients were: 0.90, 0.81 and 0.96, respectively [71].*

676 4.2.4. From cellulose hydrolysis to real biomass hydrolysis in
 677 supercritical water

678 Then, once all the parameters affecting cellulose hydrolysis/dissolution were
 679 revised, it is worth mentioning that the key parameters to selectively hydrolyze
 680 cellulose and therefore biomass in supercritical water are the effective control of
 681 reaction time and the medium properties. As the hydrolysis rate of cellulose is
 682 higher than the glucose under supercritical conditions [68], effectively stopping
 683 the reaction after cellulose hydrolysis but before glucose degradation is essential

684 to obtain high sugar yields. Increasing the reaction time would only produce the
685 degradation of the glucose generated. In order to avoid glucose degradation
686 when working above the critical point of water, reaction times below 1 seconds
687 should be selected [67]. It was also found that both cellulose [71] and H⁺/OH⁻ ions
688 [76] concentrations should be taken into account in kinetic equations in order to
689 better explain the performance of cellulose hydrolysis in supercritical water. The
690 studies of hydrolysis of cellulose in supercritical water demonstrated that this
691 technology is very promising to obtain mono and oligo-saccharides from
692 cellulose. Working with very short reaction times (lower than 1 second) it was
693 possible to obtain high yields of sugars and low degradation products content. In
694 fact, this technology already proved to be an effective method not only for pure
695 cellulose hydrolysis but also for complex biomass hydrolysis, such as wheat bran
696 [80] and sugar beet pulp [81]. Working with the continuous sudden expansion
697 micro-reactor mentioned above, it was possible to obtain both sugars and building
698 blocks (as glycolaldehyde [43,44]) just by changing the reaction time. When
699 working with wheat bran, the highest recovery of cellulose and hemicellulose as
700 soluble sugars was 73 % w/w operating at 400 °C, 25 MPa and 0.19 s of reaction
701 time. On the other hand, starting with sugar beet pulp as raw material, working at
702 similar conditions (400 °C, 25 MPa and 0.2 s), a significant amount of
703 glycolaldehyde (more than 10% w/w) was produced apart from sugars. That
704 effluent after supercritical water hydrolysis containing sugars and glycolaldehyde
705 was then hydrogenated over Ru/MCM-48 catalyst obtaining hexitols and ethylene
706 glycol as products. It is clear that working with a real biomass implies not only
707 dealing with cellulose, but also with hemicellulose, pectins, lignin, proteins, etc.
708 The intricate matrix formed by all those polymers in plant cell wall makes cellulose
709 and hemicellulose less accessible for hydrolysis and therefore, higher reaction
710 time are needed in order to hydrolyze them into sugars. That would explain the
711 need to move optimal conditions from 0.015 s for pure cellulose hydrolysis to 0.2
712 s for biomass hydrolysis in supercritical water. That increase on reaction time
713 promotes the appearance of other compounds such as glycolaldehyde.
714 Therefore, through supercritical water hydrolysis of cellulose and biomass it was
715 possible to obtain high yields of sugars and building blocks for further production
716 of added value compounds, just by changing the reaction time.

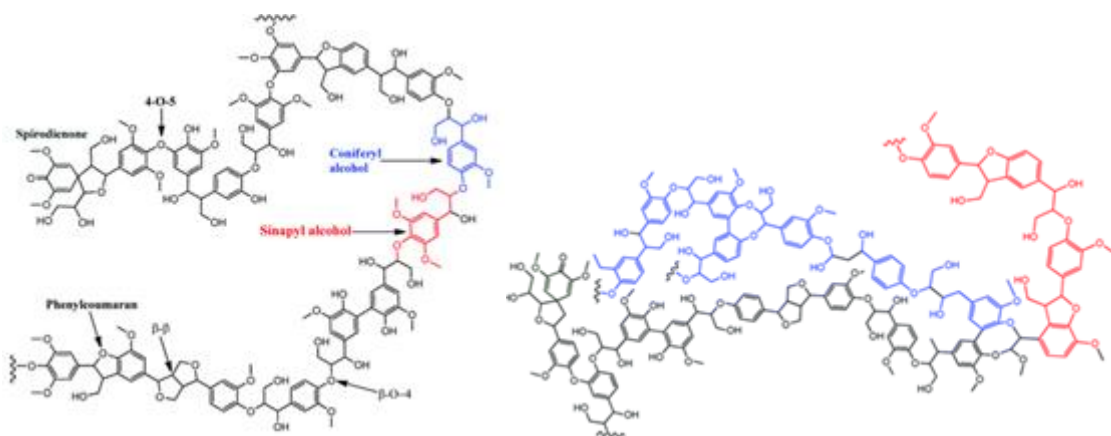
717

718

719 5. Lignin

720 Lignin, after cellulose, is the second most abundant raw material of organics [82].
721 However, lignin is still under use compared to other biomass products due to its
722 difficult decomposition and the high amounts of solid residue obtained during its
723 depolymerization [83].

724 Traditionally, lignin has been considered as a low value by-product of the pulping
725 industry. Only 2% of lignin isolated from spent pulping liquor is used for
726 specialties [84]. In spite of its amorphous and highly branched structure, it is
727 widely accepted that lignin structure comes from the polymerization of three
728 phenylpropane monomer units, namely coniferyl, synapyl, and p-coumaryl
729 alcohol [85]. These monolignols produce guaiacyl, syringyl and p-hydroxyphenyl
730 propanoic units into the lignin polymer. These substituted phenols yield a huge
731 number of functional groups and linkages, which vary from species to species,
732 tree to tree, and even in woods from different parts of the same tree [83]. Lignin
733 structure is also influenced by environmental and developmental cues [86]. For
734 instance, hardwood lignins are primarily composed by guaiacyl and syringyl units
735 with traces of p-hydroxyphenyl propanoid units, whereas softwood lignins are
736 composed mainly of guaiacyl units with low levels of p-hydroxyphenyl propanoid
737 units. The theoretical structure of hardwood and softwood lignins, is shown in
738 Figure 12.



739

740 *Figure 12. Typical structure of lignin derived from hardwood (left) and softwood*
741 *(right) [87]*

742 Despite its non-well known structure, it suggests that lignin can be a valuable
743 source of chemicals if would be broken into smaller molecular units.
744 Depolymerization of lignin is an alluring route to an important functionality class.
745 Unfortunately, nowadays this route is deceptive. Despite a large volume of
746 research, there are very few reports of efficient ways of recovering such as high
747 value-added products. Thus, if it would be possible to carry out the lignin
748 depolymerization with high yields, lignin would increase its potential as valuable
749 chemicals source, making more competent the lignocellulosic biorefinery with the
750 efficient use of the main three components of biomass, and not only cellulose and
751 hemicellulose as until now. Recently, the hydrolysis of lignin and its model
752 compounds (vanillic acid, guaiacol, syringol, coniferyl and synapyl alcohol) in sub
753 and supercritical water is being considered as a probable pathway in lignin
754 depolymerization. As is well known, the hydrolysis process has some advantages
755 compared to other methods, it is performed at lower temperatures, the employed
756 reactants are cheap and favors higher yields of liquid including monomeric
757 phenols [88].

758 5.1. Model compounds

759 The hydrothermolysis of vanillic acid (VA) was studied using a tubular flow
760 reactor, with residence times from 5 to 70 seconds, between 300 and 375 °C. It
761 was found that below the critical temperature of water, VA was converted
762 exclusively to 2-methoxy-phenol (guaiacol) through decarboxylation. At 350°C
763 the conversion was achieved faster (after only 15 s) than at 300°C (60 s). At
764 temperatures of 375 °C the conversion was even more rapid, but the selectivity
765 towards guaiacol was lower, with catechol being formed as the main secondary
766 product. Phenol was also formed, through the free radical decomposition of
767 guaiacol. As the temperature was increased further, more of the secondary
768 products were formed [89].

769 Guaiacol decomposition in supercritical water was investigated in sealed reactors
770 using both water and in water-salt solutions (NaCl, CaCl₂ and FeCl₃). The
771 reaction temperature was 383 °C with reaction times between 0 and 30 minutes.
772 It was concluded that at low water density, the reactions led to the formation of
773 phenol, catechol, cresol and char, but at higher water densities and with addition

774 of salts the rate of hydrolysis and the selectivity towards hydrolysis products,
775 catechol and methanol, was increased [90]. On the other hand, it was also
776 investigated batch reactions of guaiacol using a 5 ml reactor with residence times
777 between 5 and 180 minutes (including 3 minutes of heating up), at 380, 390 and
778 400 °C. The main products were catechol, phenol and o-cresol. Catechol was
779 formed quickly over the first 10 minutes of the reaction. Phenol and o-cresol were
780 both formed gradually over the entire reaction time [91] .

781 Formation of formic and acetic acid from syringol decomposition was studied
782 under oxidizing conditions in a batch reactor, with and without NaOH catalyst.
783 Reaction times of 30 to 150 seconds and temperatures between 250 and 300 °C
784 were investigated. NaOH had been shown to inhibit the decomposition of organic
785 compounds at these temperatures. The phenolic compounds formed were
786 catechol, 1, 2, 4-benzenetriol, 1, 4 benzenediol and 9 short chain carboxylic
787 acids, ranging from 1-6 carbons. The optimal temperature for formic and acetic
788 acid production was 280 °C though this led to a lower formation of other products
789 [92].

790 The formation of organic acids from the decomposition of coniferyl and synapyl
791 alcohols using a batch reactor at 380 °C, 1000 bar and 4 minutes was
792 investigated. Coniferyl and synapyl alcohols formed formic, acetic, glycolic and
793 lactic acid. It was suggested that these were formed from decomposition of the
794 aliphatic side chains, being the aromatic rings resistant to ring opening reactions
795 under these reaction conditions [93].

796 5.2. Lignin Depolymerization

797

798 5.2.1. Reactions in water and co-solvent

799 Existence of the additional hydrolysis reaction in water at elevated temperatures
800 and pressures catalyzed by H⁺ and OH⁻ should cause significantly different
801 decomposition from pyrolysis, and the associated phase behavior. As a weak-
802 polar solvent with a high value of ion product supercritical water could be a

803 possible solvent that can dissolve and hydrolyze lignin for potentially production
804 of phenolic chemicals or for upgrading lignin for fuels [94].

805 *Saisu et al.* reported the decomposition of organosolv lignin in a batch reactor in
806 supercritical water with and without phenol at 400 °C. As properties of lignin
807 depend on the lignin origin, not just on the isolation way, it is important to
808 emphasize that in this work authors did not give additional information about the
809 lignin origin. Both the lignin to phenol ratios and the volume of water in the reactor
810 were varied in order to investigate the effect of phenol and water density.
811 Residence times were 10-64 minutes. The reaction products were separated into
812 THF soluble (TS) and THF insoluble (TIS) fractions. In the absence of phenol it
813 was found that the molecular weight distribution of TS products shifted to lower
814 molecular weight as the water density increased. The TS products (syringols,
815 guaiacols and catechol) were derived from lignin structure. Authors explained that
816 the conversion of lignin in supercritical water probably proceeded through
817 hydrolysis and dealkylation, which leads to the formation of lighter fraction, such
818 as alcohols, aldehydes and their functional groups within the macromolecules.
819 The functional groups could form not only as decomposed fragments but also as
820 lignin itself. In the presence of phenol, there was a lower yield of TIS products,
821 which were also of a lower mass. The yield of TS increased and their average
822 mass also decreased. This can be rationalized by enhanced hydrolysis of lignin
823 at high water density, which produces reactive fragments such as formaldehyde.
824 In the absence of phenol, these reactive fragments act as cross linkers between
825 depolymerization products such as guaiacol, catechol, and larger fragments of
826 lignin, repolymerising the lignin molecule. It is believed that phenol acts as a
827 capping agent by reacting with these species to prevent the repolymerization and
828 the formation of the TIS molecules [95].

829 *Okuda et al.* studied the depolymerization of organosolv lignin in phenol-water
830 mixtures at 400 °C for 6-60 minutes. As in previous work, the information about
831 lignin origin is not given. In this study they were focused on the production of
832 phenolic chemicals from lignin and examined the depolymerization of lignin in a
833 water-phenol mixture with higher phenol ratio in order to assess the possibility of
834 complete conversion of lignin to phenolic chemicals without the formation of char.
835 It was found that the yield of TS compounds decreased with time, and after 1

836 hour the lowest yield was given when just water was used as solvent. The best
837 performing solvent was a water-phenol mixture, which achieved nearly total
838 suppression of char formation with 99% TS molecules [96].

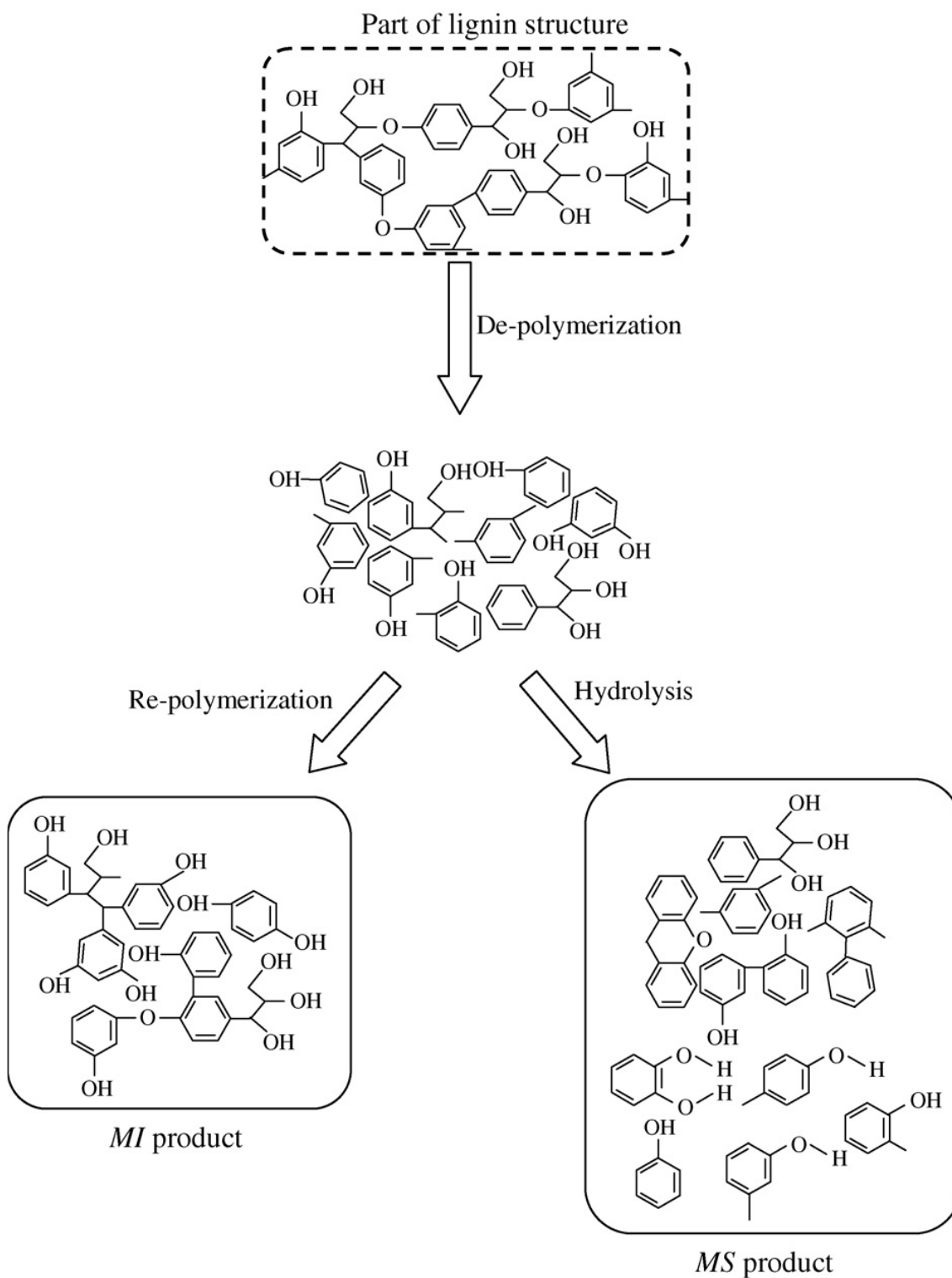
839 *Fang at al.* followed decomposition of organosolv lignin in water/phenol solution
840 in micro-reactor coupled with optical microscopies at temperatures up to 600°C
841 and water densities up to 1165 kg/m³. **The microreactor, diamond anvil cell (DAC)**
842 **allows for in-situ observations of samples in the fully-visible chamber via optical**
843 **microscopy. The DAC consisted of a hole and sealed by compression of two**
844 **opposing anvils made of diamond. The chamber was rapidly heated by two**
845 **electric microheaters by cutting power, which is convenient for the study of phase**
846 **behavior and chemical reactions.** Experiments have been done at different water
847 densities, heating rate, maximum temperatures and lignin concentration. Three
848 different types of products were obtained: a non-dissolved black residue, a
849 precipitated residue and reddish oil. A homogenous phase was formed for the
850 phenol + lignin system where phenolic char precipitated as the main product.
851 Adding water to this system de-polymerization of lignin was promoted by
852 hydrolysis in a homogeneous phase and its re-polymerization was inhibited by
853 phenol. The homogenous phase was not found in the case of lignin + water
854 system. After initial dissolution at above 377 °C lignin underwent hydrolysis and
855 pyrolysis to phenolic, which are further changed to oil in the aqueous phase. At
856 higher temperatures, solid particles precipitated from the aqueous via
857 homogeneous re-polymerization of the phenolics and water soluble compounds
858 to form a phenolic char. At these same conditions, non-dissolved lignin underwent
859 heterogeneous pyrolysis and formed polyaromatic char. Higher water density
860 decrease lignin dissolution. Therefore, polyaromatic char, with a lighter molecular
861 weight was the main product along with a smaller fraction of phenolic char. It can
862 be conclude that for water and phenol mixtures, lignin can be completely
863 solubilized and undergoes homogeneous hydrolysis and pyrolysis that prevents
864 further re-polymerization [94].

865 5.2.2. Water without co-solvent

866 *Sasaki and Goto* presented a work in which the chemical conversion of alkali
867 lignin in near and supercritical water at 350 °C and 400 °C and a pressure of 25-

868 40 MPa using a batch reactor without catalyst, having 5-240 minutes residence
869 time was studied. The products were separated into two fractions, methanol
870 soluble (MS) and methanol insoluble (MI). The main products observed in the MS
871 fraction were catechol, phenol, and o, m, p- cresols, while MI product was defined
872 as a residual solid. It was proposed that catechol is formed via hydrolysis of
873 guaiacol which is the main compound in structure of lignin. In further hydrolysis,
874 phenol, m, p and o-cresol were obtained. Dependence of reaction time showed
875 that the yield of catechol rapidly increased with reaction time (till 30 min) and then
876 decreased, especially at 400 °C, while the yields of phenol, m, p and o-cresol
877 increased with reaction time. After 90 min the yields of m, p and o-cresols were
878 almost constant while the yield of phenol slightly increased. At 400 °C after
879 catechol was consumed, the majority of the reaction most likely terminated. The
880 decreasing of catechol was not followed by the increasing of phenol, m, p and o-
881 cresol significantly. Water density influence yields of products where the yield of
882 catechol was gradually decreased with increasing the water density at 350 °C
883 and dramatically decreased at 400 °C. The yields of phenol, m, p and o-cresol
884 increased gradually with increasing the water density at 350 °C and 400 °C. It
885 was suggested that an increase in water density enhanced the hydrolysis rate of
886 ether and carbon-carbon bonds of alkylphenol in lignin. According to this results
887 it was proposed reaction mechanism showed in scheme below (Figure 13) where
888 lignin was degraded into its derivate compounds by dealkylation and hydrolysis
889 reaction. Under SCW conditions hydrolysis takes place at ether and ester bonds
890 in lignin. Hydrolysis is accelerated by a high ion product of water. Dealkylation of
891 lignin gives catechol, which is then hydrolyzed into phenol. This reaction pathway
892 suggests that some useful chemical intermediates (MS fraction) might be
893 recovered in a rapid and selective manner by changing the temperature, reaction
894 time under near and supercritical water condition. At the same time, re-
895 polymerization of low molecular weight compounds occurs as seen by the
896 formation of char through condensation reaction [97].

897



898

899

900

Figure 13. Proposed scheme for degradation of lignin under near and supercritical condition

901

902

903

Lignin conversion was also investigated in the continuous system for short residence time 0.5-10 s, pressure of 25 MPa and different temperatures under supercritical conditions at 390 °C and 450 °C and subcritical condition at 300 °C

904 and 370 °C [98] [99]. Temperature plays an important factor in deciding the
905 dominant pathway because of the existence of the parallel ionic and radical based
906 pathways. Lignin products were divided in char, gas, TOC, phenolic and aromatic
907 hydrocarbons. Under hydrothermal condition lignin was rapidly converted into
908 lower molecular weight products for all temperatures which was followed with
909 high yields of TOC, phenolic compounds and aromatic hydrocarbons, while
910 decomposition was accelerated under supercritical condition [99]. Increasing
911 decomposition rate with temperature follows Arrhenius behavior of lignin
912 degradation what was already obtained by *Zhang and Ramaswamy* [100]. The
913 rapid depolymerization is cause by cleavage of ether bonds from abundant β -aryl
914 ether (β -O-4) linkages in softwood lignin [101] [102]. The low dissociation
915 enthalpies of the ether bond in the β -O-4 linkage initiated the reaction to form a
916 phenoxy radical and a secondary alkyl aromatic radical [103]. The Arrhenius
917 behavior shown by lignin decomposition under hydrothermal conditions even in
918 subcritical region further supported the conclusion that the initial decomposition
919 was a radical reaction. TOC yield decreased with temperature and the yield was
920 much higher under subcritical condition. The TOC yield in subcritical water
921 increased within short residence time and remained stable or decrease slowly
922 despite longer residence time. The increasing in the polymerization during the
923 increase of temperature should be reflected in the TOC yield. Low TOC yield
924 under supercritical condition suggested the occurrence of secondary reaction.
925 This could be due to the cross-linking between reactive degradation fragments
926 obtained from the lignin depolymerization to produce fragments with higher
927 molecular weights. Increase in the lower molecular weight compounds during the
928 time resulted with the simultaneous formation of the higher molecular weight
929 compounds because of the repolymerization. The minimal decrease in TOC yield
930 for subcritical temperatures implied that the crosslinking reactions between these
931 lower-molecular weight compounds did not take place actively under these
932 conditions. This suggested the significance of radical's involvement in enhancing
933 the reaction [98][99].

934 Char has significantly higher yields in the supercritical region and formation was
935 enhanced at elevated temperatures. Formation of char from lignin follows
936 Arrhenius behavior and it is not affected with change in water properties under

937 subcritical condition what point radical reaction. In order to examine the
938 suggested hypothesis of formation of low molecular-weight fragments and
939 formation of higher molecular weight fragments by cross linking of the smaller
940 fragment it was determine the yields of the phenolic compounds and aromatic
941 hydrocarbons. The main phenolic compound from lignin decomposition is
942 guaiacol, which is followed by minor composition of other phenolic compounds
943 such as o, m, p-cresol, catechol and phenol. Formation of guaiacol was higher in
944 supercritical temperature, but rapidly decreased at longer residence time [98]
945 [99]. Guaiacol is an intermediate degradation product and highly reactive, since
946 the methyl C–O bond is the weakest in the guaiacol unit and is susceptible to
947 undergo cleaving. The aliphatic C–O bond of the methoxyl group is more likely to
948 react because the bond energy of the aliphatic C–O bond (245 kJ/mol) is smaller
949 than that of the aromatic C–O bond (256 kJ/mol). This was concluded in the study
950 of *Wahyudiono et al.* where also was found that guaiacol showed a fast
951 decomposition rate and the formation of high-molecular-weight substances
952 reformed to char was important for the guaiacol decomposition to reach
953 equilibrium [104]. However, high yield of guaiacol was also obtained under
954 subcritical conditions. The high yield of guaiacol under two separate regions of
955 temperature (subcritical and supercritical) with different water properties
956 indicated guaiacol formation via two different pathways. The formation of guaiacol
957 from lignin probably proceeded through hydrolysis under subcritical conditions
958 because of the high ionic product and dielectric constant of water. On the
959 contrary, under supercritical condition and high temperature free radical reaction
960 should be enhanced that lead to the formation of guaiacol from lignin [98]. In both
961 studies it was showed that the decomposition of lignin occurred rapidly with
962 residence time below one second, which indicate that kinetic study should be
963 done for residence time below 1s.

964 5.2.3. Water and base catalyst

965 In order to enhance the obtaining of monomeric phenols, basic compounds such
966 as hydroxides are used as catalyst [105][106] [107]. Studies on lignin model
967 compound dihydro-diisoeugenol, showed that the basic agent caused ether and
968 C–C bond cleavage which yielded volatile phenols [108]. Furthermore, the

969 analysis of products from model compound reactions revealed that phenyl ether
970 linkages were effectively broken in the base catalyzed hydrolysis reaction while
971 C-C linkages were less affected [109]. In another study, it was concluded that in
972 alkaline depolymerisation of lignin, ether bonds are hydrolyzed at random, most
973 likely from the outside of the oligomer and not in the sequence of their bond
974 strengths, forming first large units and then smaller subunits [106]. In addition, it
975 was stated that the formation of monomers is directly proportional to the
976 concentration of sodium hydroxide in the aqueous medium. Furthermore, a
977 mechanism for the NaOH catalyzed breakdown of the ether bonds of lignin is
978 proposed explaining the preferential formation of syringol derivatives, based on
979 the stabilizing effect that the methoxyl groups provides to the transition states of
980 the carbenium ions. It was also concluded that the production of monomers is
981 limited by the oligomerization and polymerization reactions of the products
982 formed.

983 *Miller et al.* showed that in the alkali depolymerization of lignin using water as
984 solvent the most important factor in lignin depolymerization was base
985 concentration. Moreover, it was observed that concentration excess of a strong
986 base gave better results on lignin depolymerization. In addition, a little amount of
987 a strong base (NaOH) together with a larger amount of less expensive base
988 ($\text{Ca}(\text{OH})_2$) produced positive results [105].

989 *Silva et al.* studied the catalytic depolymerization of organosolv lignin with both
990 NaOH catalyst and with boric acid as a capping agent, aiming to produce oils of
991 monomeric and dimeric products. In the case of reactions with NaOH and no
992 capping agent, the highest oil yield was obtained at 300 °C with a residence time
993 of 4 minutes. This gave a yield of 23% oil and no char formation. Lignin
994 conversion increased steadily with increasing temperature but char was formed
995 as well as oil. In order to increase oil yields, boric acid was used as a capping
996 agent. Without base, the boric acid increased the yield of oils to a maximum of
997 36% after 40 minutes at 300 °C, but at longer residence times or higher
998 temperatures the yield decreased again. The results showed that the molecular
999 weights of the oils from the boric acid catalyzed reactions were around 500 Da,
1000 compared to 300 Da for the base catalyzed depolymerization [88].

1001 In contrast to a basic environment, leading to deprotonation of phenolic hydroxyl
1002 groups and decreased hydrogen bonding, the acidic environment enhances the
1003 degree of internal hydrogen bonding. As result, the probability of acid-catalyzed
1004 cleavage of ether bonds is reduced compared to base-catalyzed cleavage. Thus,
1005 in acid-catalyzed hydrolysis the primary products produced are larger (dimers to
1006 tetramers) than in the base-catalyzed route. For both cases, the primary products
1007 undergo easy addition and condensation reactions leading to higher molecular
1008 weight products [110].

1009 Under supercritical and subcritical condition lignin is hydrolyzed and different
1010 phenolic and other aromatic compounds could be obtained. These hydrolysis
1011 reactions occur in the shortest time than the residence time that has already been
1012 used in literature (more than one second). It is very important to have better
1013 understanding of reaction pathways, intermediate reaction products and reaction
1014 products for first milliseconds of reaction time, thus the specific weaknesses and
1015 strengths of the polymer and its intermediates – i.e. the substructures which are
1016 the most susceptible to chemical attack. Kinetic models that have been obtained
1017 until today are justified with the final reaction products, without information about
1018 intermediate produced.

1019 Considerable effort is still required to address the separation challenges
1020 associated with lignin depolymerization. The supercritical water ultrafast
1021 hydrolysis could open a new way to improve the understanding of lignin
1022 depolymerization, as has been done in the cellulose hydrolysis.

1023

1024 **Acknowledgements**

1025 The authors thank MINECO and FEDER program for the financial support
1026 Projects CTQ2013-44143-R and CTQ2016-79777-R.

1027

1028

1029

1030

1031

1032

1033

1034 **References:**

- 1035 [1] P. Bajpai, Structure of Lignocellulosic Biomass, in: Pretreat. Lignocellul.
1036 Biomass Biofuel Prod., Springer Singapore, Singapore, 2016: pp. 7–12.
1037 doi:10.1007/978-981-10-0687-6_2.
- 1038 [2] O. Bobleter, Hydrothermal degradation of polymers derived from plants,
1039 Prog. Polym. Sci. 19 (1994) 797–841.
1040 <http://cat.inist.fr/?aModele=afficheN%7B&%7Dcpsidt=4247470>.
- 1041 [3] J. V Rissanen, H. Grénman, C. Xu, S. Willför, D.Y. Murzin, T. Salmi,
1042 Obtaining Spruce Hemicelluloses of Desired Molar Mass by using
1043 Pressurized Hot Water Extraction, ChemSusChem. 7 (2014) 2947–2953.
1044 doi:10.1002/cssc.201402282.
- 1045 [4] G. Gallina, Á. Cabeza, P. Biasi, J. García-Serna, Optimal conditions for
1046 hemicelluloses extraction from Eucalyptus globulus wood: hydrothermal
1047 treatment in a semi-continuous reactor, Fuel Process. Technol. 148
1048 (2016) 350–360. doi:<http://doi.org/10.1016/j.fuproc.2016.03.018>.
- 1049 [5] C. Wyman, S. Decker, M. Himmel, J. Brady, C. Skopec, L. Viikari,
1050 Hydrolysis of Cellulose and Hemicellulose, in: Polysaccharides, CRC
1051 Press, 2004. doi:doi:10.1201/9781420030822.ch43.
- 1052 [6] A. Cabeza, C.M. Piqueras, F. Sobrón, J. García-Serna, Modeling of
1053 biomass fractionation in a lab-scale biorefinery: Solubilization of
1054 hemicellulose and cellulose from holm oak wood using subcritical water,
1055 Bioresour. Technol. 200 (2016) 90–102.
1056 doi:<http://doi.org/10.1016/j.biortech.2015.09.063>.
- 1057 [7] F. Carneiro, L.C. Duarte, F. Gírio, P. Moniz, Chapter 14 -
1058 Hydrothermal/Liquid Hot Water Pretreatment (Autohydrolysis):
1059 A Multipurpose Process for Biomass Upgrading A2 - Mussatto, Solange I,
1060 in: Biomass Fractionation Technol. a Lignocellul. Feed. Based Biorefinery,
1061 Elsevier, Amsterdam, 2016: pp. 315–347. doi:<http://doi.org/10.1016/B978-0-12-802323-5.00014-1>.

- 1063 [8] C.M. Piqueras, Á. Cabeza, G. Gallina, D.A. Cantero, J. García-Serna,
1064 M.J. Cocero, Online integrated fractionation-hydrolysis of lignocellulosic
1065 biomass using sub- and supercritical water, *Chem. Eng. J.* 308 (2017)
1066 110–125. doi:<http://doi.org/10.1016/j.cej.2016.09.007>.
- 1067 [9] F.M. Yedro, H. Grénman, J. V Rissanen, T. Salmi, J. García-Serna, M.J.
1068 Cocero, Chemical composition and extraction kinetics of Holm oak
1069 (*Quercus ilex*) hemicelluloses using subcritical water, *J. Supercrit. Fluids.*
1070 (n.d.). doi:<http://doi.org/10.1016/j.supflu.2017.01.016>.
- 1071 [10] J. V Rissanen, H. Grénman, S. Willför, D.Y. Murzin, T. Salmi, Spruce
1072 Hemicellulose for Chemicals Using Aqueous Extraction: Kinetics, Mass
1073 Transfer, and Modeling, *Ind. Eng. Chem. Res.* 53 (2014) 6341–6350.
1074 doi:10.1021/ie500234t.
- 1075 [11] B. Sukhbaatar, E.B. Hassan, M. Kim, P. Steele, L. Ingram, Optimization of
1076 hot-compressed water pretreatment of bagasse and characterization of
1077 extracted hemicelluloses, *Carbohydr. Polym.* 101 (2014) 196–202.
1078 doi:<http://doi.org/10.1016/j.carbpol.2013.09.027>.
- 1079 [12] J. V Rissanen, D.Y. Murzin, T. Salmi, H. Grénman, Aqueous extraction of
1080 hemicelluloses from spruce – From hot to warm, *Bioresour. Technol.* 199
1081 (2016) 279–282. doi:<http://doi.org/10.1016/j.biortech.2015.08.116>.
- 1082 [13] W. Reynolds, H. Singer, S. Schug, I. Smirnova, Hydrothermal flow-
1083 through treatment of wheat-straw: Detailed characterization of fixed-bed
1084 properties and axial dispersion, *Chem. Eng. J.* 281 (2015) 696–703.
1085 doi:<http://doi.org/10.1016/j.cej.2015.06.117>.
- 1086 [14] A. Cabeza, F. Sobrón, F.M. Yedro, J. García-Serna, Two-phase
1087 modelling and simulation of the hydrothermal fractionation of holm oak in
1088 a packed bed reactor with hot pressurized water, *Chem. Eng. Sci.* 138
1089 (2015) 59–70. doi:<http://doi.org/10.1016/j.ces.2015.07.024>.
- 1090 [15] X. Chen, M. Lawoko, A. van Heiningen, Kinetics and mechanism of
1091 autohydrolysis of hardwoods, *Bioresour. Technol.* 101 (2010) 7812–7819.
1092 doi:<http://doi.org/10.1016/j.biortech.2010.05.006>.
- 1093 [16] X.J. Ma, X.F. Yang, X. Zheng, L. Lin, L.H. Chen, L.L. Huang, S.L. Cao,
1094 Degradation and dissolution of hemicelluloses during bamboo

- 1095 hydrothermal pretreatment, *Bioresour. Technol.* 161 (2014) 215–220.
1096 doi:<http://doi.org/10.1016/j.biortech.2014.03.044>.
- 1097 [17] M.E. Vallejos, F.E. Felissia, J. Kruyeniski, M.C. Area, Kinetic study of the
1098 extraction of hemicellulosic carbohydrates from sugarcane bagasse by
1099 hot water treatment, *Ind. Crops Prod.* 67 (2015) 1–6.
1100 doi:<http://doi.org/10.1016/j.indcrop.2014.12.058>.
- 1101 [18] M.H. Thomsen, A. Thygesen, A.B. Thomsen, Hydrothermal treatment of
1102 wheat straw at pilot plant scale using a three-step reactor system aiming
1103 at high hemicellulose recovery, high cellulose digestibility and low lignin
1104 hydrolysis, *Bioresour. Technol.* 99 (2008) 4221–4228.
1105 <http://linkinghub.elsevier.com/retrieve/pii/S0960852407007158>.
- 1106 [19] M.S.R. dos Santos Rocha, B. Pratto, R. de Sousa Júnior, R.M.R.G.
1107 Almeida, A.J.G. da Cruz, A kinetic model for hydrothermal pretreatment of
1108 sugarcane straw, *Bioresour. Technol.* 228 (2017) 176–185.
1109 doi:<http://doi.org/10.1016/j.biortech.2016.12.087>.
- 1110 [20] S. Makishima, M. Mizuno, N. Sato, K. Shinji, M. Suzuki, K. Nozaki, F.
1111 Takahashi, T. Kanda, Y. Amano, Development of continuous flow type
1112 hydrothermal reactor for hemicellulose fraction recovery from corncob,
1113 *Bioresour. Technol.* 100 (2009) 2842–2848.
1114 <http://linkinghub.elsevier.com/retrieve/pii/S0960852408010791>.
- 1115 [21] A. Eseyin E., P. Steele H., An overview of the applications of furfural and
1116 its derivatives, 2015. 3 (2015) 6. doi:10.14419/ijac.v3i2.5048.
- 1117 [22] F.A. Castillo Martinez, E.M. Balciunas, J.M. Salgado, J.M. Domínguez
1118 González, A. Converti, R.P. de S. Oliveira, Lactic acid properties,
1119 applications and production: A review, *Trends Food Sci. Technol.* 30
1120 (2013) 70–83. doi:<https://doi.org/10.1016/j.tifs.2012.11.007>.
- 1121 [23] P. Gao, G. Li, F. Yang, X.-N. Lv, H. Fan, L. Meng, X.-Q. Yu, Preparation
1122 of lactic acid, formic acid and acetic acid from cotton cellulose by the
1123 alkaline pre-treatment and hydrothermal degradation, *Ind. Crops Prod.* 48
1124 (2013) 61–67. doi:<http://doi.org/10.1016/j.indcrop.2013.04.002>.
- 1125 [24] J.C. Parajó, G. Garrote, J.M. Cruz, H. Dominguez, Production of
1126 xylooligosaccharides by autohydrolysis of lignocellulosic materials,

- 1127 Trends Food Sci. {&} Technol. 15 (2004) 115–120.
1128 <http://linkinghub.elsevier.com/retrieve/pii/S0924224403002553>.
- 1129 [25] G. Garrote, H. Domínguez, J.C. Parajó, Interpretation of deacetylation
1130 and hemicellulose hydrolysis during hydrothermal treatments on the basis
1131 of the severity factor, *Process Biochem.* 37 (2002) 1067–1073.
1132 doi:[http://doi.org/10.1016/S0032-9592\(01\)00315-6](http://doi.org/10.1016/S0032-9592(01)00315-6).
- 1133 [26] M.R. Narkhede, C. Nguyen-Trung, D.A. Palmer, Dissociation quotients of
1134 D-galacturonic acid in aqueous solution at 0.1 MPa to 1 molal ionic
1135 strength and 100°C, *J. Solution Chem.* 23 (1994) 877–888.
1136 doi:[10.1007/bf00972751](https://doi.org/10.1007/bf00972751).
- 1137 [27] M.S. Tunc, A.R.P. van Heiningen, Hemicellulose Extraction of Mixed
1138 Southern Hardwood with Water at 150 °C: Effect of Time, *Ind. {&} Eng.
1139 Chem. Res.* 47 (2008) 7031–7037.
1140 <http://pubs.acs.org/doi/abs/10.1021/ie8007105>.
- 1141 [28] T. Song, A. Pranovich, B. Holmbom, Effects of pH control with phthalate
1142 buffers on hot-water extraction of hemicelluloses from spruce wood,
1143 *Bioresour. Technol.* 102 (2011) 10518–10523.
1144 doi:<http://doi.org/10.1016/j.biortech.2011.08.093>.
- 1145 [29] H.A. Ruiz, M.A. Cerqueira, H.D. Silva, R.M. Rodríguez-Jasso, A.A.
1146 Vicente, J.A. Teixeira, Biorefinery valorization of autohydrolysis wheat
1147 straw hemicellulose to be applied in a polymer-blend film, *Carbohydr.
1148 Polym.* 92 (2013) 2154–2162.
1149 doi:<http://doi.org/10.1016/j.carbpol.2012.11.054>.
- 1150 [30] G. Brunner, Chapter 8 - Processing of Biomass with Hydrothermal and
1151 Supercritical Water, in: B. Gerd (Ed.), *Supercrit. Fluid Sci. Technol.*,
1152 Elsevier, 2014: pp. 395–509.
1153 <http://www.sciencedirect.com/science/article/pii/B978044459413600008X>.
- 1154 [31] F.M. Yedro, D.A. Cantero, M. Pascual, J. García-serna, M.J. Cocero,
1155 *Bioresource Technology* Hydrothermal fractionation of woody biomass :
1156 Lignin effect on sugars recovery, *Bioresour. Technol.* 191 (2015) 124–
1157 132. doi:[10.1016/j.biortech.2015.05.004](https://doi.org/10.1016/j.biortech.2015.05.004).
- 1158 [32] H.A. Ruiz, R.M. Rodr??guez-Jasso, B.D. Fernandes, A.A. Vicente, J.A.

- 1159 Teixeira, Hydrothermal processing, as an alternative for upgrading
1160 agriculture residues and marine biomass according to the biorefinery
1161 concept: A review, *Renew. Sustain. Energy Rev.* 21 (2013) 35–51.
1162 doi:10.1016/j.rser.2012.11.069.
- 1163 [33] H.-Q. Li, W. Jiang, J.-X. Jia, J. Xu, pH pre-corrected liquid hot water
1164 pretreatment on corn stover with high hemicellulose recovery and low
1165 inhibitors formation, *Bioresour. Technol.* 153 (2014) 292–299.
1166 doi:<https://doi.org/10.1016/j.biortech.2013.11.089>.
- 1167 [34] S. Ou, K.-C. Kwok, Ferulic acid: pharmaceutical functions, preparation
1168 and applications in foods, *J. Sci. Food Agric.* 84 (2004) 1261–1269.
1169 doi:10.1002/jsfa.1873.
- 1170 [35] B.A. Acosta-Estrada, J.A. Gutierrez-Urbe, S.O. Serna-Saldivar, Bound
1171 phenolics in foods, a review, *Food Chem.* 152 (2014) 46–55.
1172 doi:10.1016/j.foodchem.2013.11.093.
- 1173 [36] N. Kumar, V. Pruthi, Potential applications of ferulic acid from natural
1174 sources, *Biotechnol. Reports.* 4 (2014) 86–93.
1175 doi:<https://doi.org/10.1016/j.btre.2014.09.002>.
- 1176 [37] K. Krygier, F. Sosulski, L. Hogge, Free, esterified, and insoluble-bound
1177 phenolic acids. 1. Extraction and purification procedure, *J. Agric. Food
1178 Chem.* 30 (1982) 330–334.
- 1179 [38] I. Benoit, D. Navarro, N. Marnet, N. Rakotomanomana, L. Lesage-
1180 Meessen, J.-C. Sigoillot, M. Asther, M. Asther, Feruloyl esterases as a
1181 tool for the release of phenolic compounds from agro-industrial by-
1182 products, *Carbohydr. Res.* 341 (2006) 1820–1827.
1183 doi:<https://doi.org/10.1016/j.carres.2006.04.020>.
- 1184 [39] H. Barberousse, A. Kamoun, M. Chaabouni, J.-M. Giet, O. Roiseux, M.
1185 Paquot, C. Deroanne, C. Blecker, Optimization of enzymatic extraction of
1186 ferulic acid from wheat bran, using response surface methodology, and
1187 characterization of the resulting fractions, *J. Sci. Food Agric.* 89 (2009)
1188 1634–1641. <http://onlinelibrary.wiley.com/doi/10.1002/jsfa.3630/abstract>.
- 1189 [40] O. Pourali, F.S. Asghari, H. Yoshida, Production of phenolic compounds
1190 from rice bran biomass under subcritical water conditions, *Chem. Eng. J.*

- 1191 160 (2010) 259–266. doi:10.1016/j.cej.2010.02.057.
- 1192 [41] R.J. Moon, A. Martini, J. Nairn, J. Simonsen, J. Youngblood, Cellulose
1193 nanomaterials review: structure{,} properties and nanocomposites, Chem.
1194 Soc. Rev. 40 (2011) 3941–3994. doi:10.1039/C0CS00108B.
- 1195 [42] Suhas, V.K. Gupta, P.J.M. Carrott, R. Singh, M. Chaudhary, S.
1196 Kushwaha, Cellulose: A review as natural, modified and activated carbon
1197 adsorbent, Bioresour. Technol. 216 (2016) 1066–1076.
1198 doi:10.1016/j.biortech.2016.05.106.
- 1199 [43] A. Wang, T. Zhang, One-Pot Conversion of Cellulose to Ethylene Glycol
1200 with Multifunctional Tungsten-Based Catalysts, Acc. Chem. Res. 46
1201 (2013) 1377–1386. doi:10.1021/ar3002156.
- 1202 [44] L. Zhang, C. Xu, P. Champagne, Overview of recent advances in thermo-
1203 chemical conversion of biomass, Energy Convers. Manag. 51 (2010)
1204 969–982.
1205 <http://www.sciencedirect.com/science/article/pii/S0196890409004889>.
- 1206 [45] D. Klemm, B. Heublein, H. Fink, A. Bohn, Cellulose: Fascinating
1207 Biopolymer and Sustainable Raw Material, Angew. Chemie Int. Ed. 44
1208 (2005) 3358–3393.
1209 <http://onlinelibrary.wiley.com/doi/10.1002/anie.200460587/abstract>.
- 1210 [46] C.-H. Zhou, X. Xia, C.-X. Lin, D.-S. Tong, J. Beltramini, Catalytic
1211 conversion of lignocellulosic biomass to fine chemicals and fuels, Chem.
1212 Soc. Rev. 40 (2011) 5588–5617. doi:10.1039/C1CS15124J.
- 1213 [47] G. Brunner, Near critical and supercritical water. Part I. Hydrolytic and
1214 hydrothermal processes, J. Supercrit. Fluids. 47 (2009) 373–381.
1215 <http://linkinghub.elsevier.com/retrieve/pii/S0896844608002970>.
- 1216 [48] B. Lindman, G. Karlström, L. Stigsson, On the mechanism of dissolution
1217 of cellulose, J. Mol. Liq. 156 (2010) 76–81.
1218 doi:10.1016/j.molliq.2010.04.016.
- 1219 [49] B. Medronho, B. Lindman, Competing forces during cellulose dissolution:
1220 From solvents to mechanisms, Curr. Opin. Colloid {&} Interface Sci. 19
1221 (2014) 32–40. doi:10.1016/j.cocis.2013.12.001.

- 1222 [50] L.K. Tolonen, M. Bergensträhle-Wohlert, H. Sixta, J. Wohlert, Solubility of
1223 Cellulose in Supercritical Water Studied by Molecular Dynamics
1224 Simulations, *J. Phys. Chem. B.* 119 (2015) 4739–4748.
1225 doi:10.1021/acs.jpcc.5b01121.
- 1226 [51] S. Deguchi, K. Tsujii, K. Horikoshi, Crystalline-to-amorphous
1227 transformation of cellulose in hot and compressed water and its
1228 implications for hydrothermal conversion, *Green Chem.* 10 (2008) 191.
1229 <http://xlink.rsc.org/?DOI=b713655b>.
- 1230 [52] C. Yamane, T. Aoyagi, M. Ago, K. Sato, K. Okajima, T. Takahashi, Two
1231 Different Surface Properties of Regenerated Cellulose due to Structural
1232 Anisotropy, *Polym. J.* 38 (2006) 819–826.
- 1233 [53] Y. Ogihara, R.L. Smith Jr., H. Inomata, K. Arai, R.L. Smith, H. Inomata, K.
1234 Arai, Direct observation of cellulose dissolution in subcritical and
1235 supercritical water over a wide range of water densities (550-1000
1236 kg/m³), *Cellulose.* 12 (2005) 595–606.
1237 <http://link.springer.com/10.1007/s10570-005-9008-1>.
- 1238 [54] L.K. Tolonen, P.A. Penttilä, R. Serimaa, H. Sixta, The yield of cellulose
1239 precipitate from sub- and supercritical water treatment of various
1240 microcrystalline celluloses, *Cellulose.* 22 (2015) 1715–1728.
1241 doi:10.1007/s10570-015-0628-9.
- 1242 [55] R. Abdullah, K. Ueda, S. Saka, Hydrothermal decomposition of various
1243 crystalline celluloses as treated by semi-flow hot-compressed water, *J.*
1244 *Wood Sci.* 60 (2014) 278–286. doi:10.1007/s10086-014-1401-7.
- 1245 [56] Y. Yu, H. Wu, Understanding the Primary Liquid Products of Cellulose
1246 Hydrolysis in Hot-Compressed Water at Various Reaction Temperatures,
1247 *Energy & Fuels.* 24 (2010) 1963–1971. doi:10.1021/ef9013746.
- 1248 [57] Y. Yu, H. Wu, Effect of ball milling on the hydrolysis of microcrystalline
1249 cellulose in hot-compressed water, *AIChE J.* 57 (2011) 793–800.
1250 doi:10.1002/aic.12288.
- 1251 [58] L.P. Novo, J. Bras, A. García, N. Belgacem, A.A.S. Curvelo, Subcritical
1252 Water: A Method for Green Production of Cellulose Nanocrystals, *ACS*
1253 *Sustain. Chem. & Eng.* 3 (2015) 2839–2846.

- 1254 doi:10.1021/acssuschemeng.5b00762.
- 1255 [59] L.K. Tolonen, P.A. Penttilä, R. Serimaa, A. Kruse, H. Sixta, The swelling
1256 and dissolution of cellulose crystallites in subcritical and supercritical
1257 water, *Cellulose*. 20 (2013) 2731–2744.
1258 <http://link.springer.com/article/10.1007/s10570-013-0072-7>.
- 1259 [60] T. Adschiri, S. Hirose, R. Malaluan, K. Arai, Noncatalytic Conversion of
1260 Cellulose in Supercritical and Subcritical Water, *J. Chem. Eng. JAPAN*.
1261 26 (1993) 676–680. doi:10.1252/jcej.26.676.
- 1262 [61] M. Sasaki, T. Adschiri, K. Arai, Production of Cellulose II from Native
1263 Cellulose by Near- and Supercritical Water Solubilization, *J. Agric. Food*
1264 *Chem.* 51 (2003) 5376–5381. doi:10.1021/jf025989i.
- 1265 [62] S. Kumar, R.B. Gupta, Hydrolysis of Microcrystalline Cellulose in
1266 Subcritical and Supercritical Water in a Continuous Flow Reactor, *Ind. {&}*
1267 *Eng. Chem. Res.* 47 (2008) 9321–9329.
1268 <http://dx.doi.org/10.1021/ie801102j>.
- 1269 [63] L.K. Tolonen, G. Zuckerstätter, P.A. Penttilä, W. Milacher, W. Habicht, R.
1270 Serimaa, A. Kruse, H. Sixta, Structural Changes in Microcrystalline
1271 Cellulose in Subcritical Water Treatment, *Biomacromolecules*. 12 (2011)
1272 2544–2551. doi:10.1021/bm200351y.
- 1273 [64] M. Mohan, R. Timung, N.N. Deshavath, T. Banerjee, V. V Goud, V. V
1274 Dasu, Optimization and hydrolysis of cellulose under subcritical water
1275 treatment for the production of total reducing sugars, *RSC Adv.* 5 (2015)
1276 103265–103275. doi:10.1039/C5RA20319H.
- 1277 [65] M.S. Seehra, B. V Popp, F. Goulay, S.K. Pyapalli, T. Gullion, J. Poston,
1278 Hydrothermal treatment of microcrystalline cellulose under mild
1279 conditions: characterization of solid and liquid-phase products, *Cellulose*.
1280 21 (2014) 4483–4495. doi:10.1007/s10570-014-0424-y.
- 1281 [66] M. Sasaki, T. Adschiri, K. Arai, Kinetics of cellulose conversion at 25 MPa
1282 in sub- and supercritical water, *AIChE J.* 50 (2004) 192–202.
1283 doi:10.1002/aic.10018.
- 1284 [67] D.A. Cantero, M. Dolores Bermejo, M. José Cocero, High glucose

- 1285 selectivity in pressurized water hydrolysis of cellulose using ultra-fast
1286 reactors, *Bioresour. Technol.* 135 (2013) 697–703.
1287 doi:10.1016/j.biortech.2012.09.035.
- 1288 [68] M. Sasaki, Z. Fang, Y. Fukushima, T. Adschiri, K. Arai, Dissolution and
1289 Hydrolysis of Cellulose in Subcritical and Supercritical Water, *Ind. Eng.*
1290 *Chem. Res.* 39 (2000) 2883–2890. <http://dx.doi.org/10.1021/ie990690j>.
- 1291 [69] L.K. Tolonen, M. Juvonen, K. Niemelä, A. Mikkelsen, M. Tenkanen, H.
1292 Sixta, Supercritical water treatment for cello-oligosaccharide production
1293 from microcrystalline cellulose, *Carbohydr. Res.* 401 (2015) 16–23.
1294 doi:10.1016/j.carres.2014.10.012.
- 1295 [70] K. Ehara, S. Saka, Decomposition behavior of cellulose in supercritical
1296 water, subcritical water, and their combined treatments, *J. Wood Sci.* 51
1297 (2005) 148–153.
1298 <http://www.springerlink.com/content/w26363n08327171w/>.
- 1299 [71] C.M. Martínez, D.A. Cantero, M.D. Bermejo, M.J. Cocero, Hydrolysis of
1300 cellulose in supercritical water: reagent concentration as a selectivity
1301 factor, *Cellulose.* 22 (2015) 2231–2243. doi:10.1007/s10570-015-0674-3.
- 1302 [72] D.A. Cantero, M.D. Bermejo, M.J. Cocero, Kinetic analysis of cellulose
1303 depolymerization reactions in near critical water, *J. Supercrit. Fluids.* 75
1304 (2013) 48–57. doi:10.1016/j.supflu.2012.12.013.
- 1305 [73] K. Ehara, S. Saka, A comparative study on chemical conversion of
1306 cellulose between the batch-type and flow-type systems in supercritical
1307 water, *Cellulose.* 9 (2002) 301–311. doi:10.1023/A:1021192711007.
- 1308 [74] Y. Zhao, W.-J. Lu, H.-T. Wang, Supercritical hydrolysis of cellulose for
1309 oligosaccharide production in combined technology, *Chem. Eng. J.* 150
1310 (2009) 411–417.
1311 <http://www.sciencedirect.com/science/article/pii/S1385894709000564>.
- 1312 [75] D.A. Cantero, Á. Sánchez Tapia, M.D. Bermejo, M.J. Cocero, Pressure
1313 and temperature effect on cellulose hydrolysis in pressurized water,
1314 *Chem. Eng. J.* 276 (2015) 145–154. doi:10.1016/j.cej.2015.04.076.
- 1315 [76] D.A. Cantero, M.D. Bermejo, M.J. Cocero, Governing Chemistry of

- 1316 Cellulose Hydrolysis in Supercritical Water, *ChemSusChem*. 8 (2015)
1317 1026–1033. doi:10.1002/cssc.201403385.
- 1318 [77] N. Akiya, P.E. Savage, Roles of Water for Chemical Reactions in High-
1319 Temperature Water, *Chem. Rev.* 102 (2002) 2725–2750.
- 1320 [78] A. Kruse, A. Gawlik, Biomass Conversion in Water at 330–410 °C and
1321 30–50 MPa. Identification of Key Compounds for Indicating Different
1322 Chemical Reaction Pathways, *Ind. {&} Eng. Chem. Res.* 42 (2003) 267–
1323 279. doi:10.1021/ie0202773.
- 1324 [79] C. Promdej, Y. Matsumura, Temperature Effect on Hydrothermal
1325 Decomposition of Glucose in Sub- And Supercritical Water, *Ind. {&} Eng.*
1326 *Chem. Res.* 50 (2011) 8492–8497.
1327 <http://pubs.acs.org/doi/abs/10.1021/ie200298c>.
- 1328 [80] D.A. Cantero, C. Martínez, M.D. Bermejo, M.J. Cocero, Simultaneous and
1329 selective recovery of cellulose and hemicellulose fractions from wheat
1330 bran by supercritical water hydrolysis, *Green Chem.* 17 (2015) 610–618.
1331 doi:10.1039/c4gc01359j.
- 1332 [81] A. Romero, D.A. Cantero, A. Nieto-Márquez, C. Martínez, E. Alonso, M.J.
1333 Cocero, Supercritical water hydrolysis of cellulosic biomass as effective
1334 pretreatment to catalytic production of hexitols and ethylene glycol over
1335 Ru/MCM-48, *Green Chem.* 18 (2016) 4051–4062.
1336 doi:10.1039/C6GC00374E.
- 1337 [82] R.J.A. Gosselink, E. De Jong, B. Guran, A. Abächerli, Co-ordination
1338 network for lignin - Standardisation, production and applications adapted
1339 to market requirements (EUROLIGNIN), *Ind. Crops Prod.* 20 (2004) 121–
1340 129. doi:10.1016/j.indcrop.2004.04.015.
- 1341 [83] M.P. Pandey, C.S. Kim, Lignin Depolymerization and Conversion: A
1342 Review of Thermochemical Methods, *Chem. Eng. Technol.* 34 (2011) 29–
1343 41. doi:10.1002/ceat.201000270.
- 1344 [84] J.H. Lora, W.G. Glasser, Recent industrial applications of lignin: A
1345 sustainable alternative to nonrenewable materials, *J. Polym. Environ.* 10
1346 (2002) 39–48. doi:10.1023/A:1021070006895.

- 1347 [85] J. Ralph, J. Peng, F. Lu, Isochroman structures in lignin: A new β -1
1348 pathway, *Tetrahedron Lett.* 39 (1998) 4963–4964. doi:10.1016/S0040-
1349 4039(98)00968-X.
- 1350 [86] M.M. Campbell, R.R. Sederoff, Variation in Lignin Content and
1351 Composition (Mechanisms of Control and Implications for the Genetic
1352 Improvement of Plants)., *Plant Physiol.* 110 (1996) 3–13.
1353 doi:10.1104/pp.110.1.3.
- 1354 [87] W.-J. Liu, H. Jiang, H.-Q. Yu, Thermochemical conversion of lignin to
1355 functional materials: a review and future directions, *Green Chem.* 17
1356 (2015) 4888–4907. doi:10.1039/C5GC01054C.
- 1357 [88] E.A.B. da Silva, M. Zabkova, J.D. Araújo, C.A. Cateto, M.F. Barreiro, M.N.
1358 Belgacem, A.E. Rodrigues, An integrated process to produce vanillin and
1359 lignin-based polyurethanes from Kraft lignin, *Chem. Eng. Res. Des.* 87
1360 (2009) 1276–1292. doi:10.1016/j.cherd.2009.05.008.
- 1361 [89] G. Gonzalez, J. Salvado, D. Montane, Reactions of vanillic acid in sub-
1362 and supercritical water, *J. Supercrit. Fluids.* 31 (2004) 57–66.
1363 doi:10.1016/j.supflu.2003.09.015.
- 1364 [90] G.L. Huppert, B.C. Wu, S.H. Townsend, M.T. Klein, S.C. Paspek,
1365 Hydrolysis in supercritical water: identification and implications of a polar
1366 transition state, *Ind. Eng. Chem. Res.* 28 (1989) 161–165.
1367 doi:10.1021/ie00086a006.
- 1368 [91] Wahyudiono, T. Kanetake, M. Sasaki, M. Goto, Decomposition of a Lignin
1369 Model Compound under Hydrothermal Conditions, *Chem. Eng. Technol.*
1370 30 (2007) 1113–1122. doi:10.1002/ceat.200700066.
- 1371 [92] L. Pan, Z. Shen, L. Wu, Y. Zhang, X. Zhou, F. Jin, Hydrothermal
1372 production of formic and acetic acids from syringol, *J. Zhejiang Univ. Sci.*
1373 *A.* 11 (2010) 613–618. doi:10.1631/jzus.A1000043.
- 1374 [93] K. Yoshida, J. Kusaki, K. Ehara, S. Saka, Characterization of low
1375 molecular weight organic acids from beech wood treated in supercritical
1376 water, *Appl. Biochem. Biotechnol.* 121–124 (2005) 795–806.
- 1377 [94] Z. Fang, T. Sato, R.L. Smith, H. Inomata, K. Arai, J.A. Kozinski, Reaction

- 1378 chemistry and phase behavior of lignin in high-temperature and
1379 supercritical water, *Bioresour. Technol.* 99 (2008) 3424–3430.
1380 doi:10.1016/j.biortech.2007.08.008.
- 1381 [95] M. Saisu, T. Sato, M. Watanabe, T. Adschiri, K. Arai, Conversion of Lignin
1382 with Supercritical Water - Phenol Mixtures, *Energy & Fuels.* (2003) 922–
1383 928.
- 1384 [96] K. Okuda, M. Umetsu, S. Takami, T. Adschiri, Disassembly of lignin and
1385 chemical recovery - Rapid depolymerization of lignin without char
1386 formation in water-phenol mixtures, *Fuel Process. Technol.* 85 (2004)
1387 803–813. doi:10.1016/j.fuproc.2003.11.027.
- 1388 [97] Wahyudiono, M. Sasaki, M. Goto, Recovery of phenolic compounds
1389 through the decomposition of lignin in near and supercritical water, *Chem.*
1390 *Eng. Process. Process Intensif.* 47 (2008) 1609–1619.
1391 doi:10.1016/j.cep.2007.09.001.
- 1392 [98] T.L.K. Yong, M. Yukihiro, Kinetic Analysis of Lignin Hydrothermal
1393 Conversion in Sub- and Supercritical Water, *Ind. Eng. Chem. Res.* 52
1394 (2013) 9048–9059.
- 1395 [99] T.L.K. Yong, Y. Matsumura, Reaction Kinetics of the Lignin Conversion in
1396 Supercritical Water, (2012) 0–8.
- 1397 [100] B. Zhang, H.J. Huang, S. Ramaswamy, Reaction kinetics of the
1398 hydrothermal treatment of lignin, *Appl. Biochem. Biotechnol.* 147 (2008)
1399 119–131. doi:10.1007/s12010-007-8070-6.
- 1400 [101] J. Li, G. Henriksson, G. Gellerstedt, Lignin
1401 depolymerization/repolymerization and its critical role for delignification of
1402 aspen wood by steam explosion, *Bioresour. Technol.* 98 (2007) 3061–
1403 3068. doi:10.1016/j.biortech.2006.10.018.
- 1404 [102] S. Kang, X. Li, J. Fan, J. Chang, Classified separation of lignin
1405 hydrothermal liquefied products, *Ind. Eng. Chem. Res.* 50 (2011) 11288–
1406 11296. doi:10.1021/ie2011356.
- 1407 [103] T. Faravelli, A. Frassoldati, G. Migliavacca, E. Ranzi, Detailed kinetic
1408 modeling of the thermal degradation of lignins, *Biomass and Bioenergy.*

- 1409 34 (2010) 290–301. doi:10.1016/j.biombioe.2009.10.018.
- 1410 [104] Wahyudiono, M. Sasaki, M. Goto, Thermal decomposition of guaiacol in
1411 sub- and supercritical water and its kinetic analysis, *J. Mater. Cycles*
1412 *Waste Manag.* 13 (2011) 68–79. doi:10.1007/s10163-010-0309-6.
- 1413 [105] J. Miller, L. Evans, J.E. Mudd, K.A. Brown, Batch microreactor studies of
1414 lignin depolymerization by bases. 2. Aqueous Solvents, *Sandia Natl. Rep.*
1415 (2002). doi:10.2172/800964.
- 1416 [106] V.M. Roberts, V. Stein, T. Reiner, A. Lemonidou, X. Li, J.A. Lercher,
1417 Towards quantitative catalytic lignin depolymerization, *Chem. - A Eur. J.*
1418 17 (2011) 5939–5948. doi:10.1002/chem.201002438.
- 1419 [107] A. Toledano, L. Serrano, J. Labidi, Organosolv lignin depolymerization
1420 with different base catalysts, *J. Chem. Technol. Biotechnol.* 87 (2012)
1421 1593–1599. doi:10.1002/jctb.3799.
- 1422 [108] B.F. Ward, Tall Oil- Chemicals from a natural, renewable source, *Proc.*
1423 *Eight Cellul. Conf. Wood Chem. Chall.* 378 (1975) 332–334.
- 1424 [109] J.E. Miller, L. Evans, A. Littlewolf, D.E. Trudell, Batch microreactor studies
1425 of lignin and lignin model compound depolymerization by bases in alcohol
1426 solvents, *Fuel.* 78 (1999) 1363–1366. doi:10.1016/S0016-2361(99)00072-
1427 1.
- 1428 [110] X.E. Iriarte, Study of lignin as high added value chemical compounds
1429 source, Thesis 2014 UPV San Sebastian Spain.

1430

1431

1432

1433

1434

1435

1436

1437

1438

1439

1440

1441 Figures captions

1442 *Figure 1: Lignocellulosic biomass structure*

1443 *Figure 2. Subcritical and supercritical water properties around the critical point.*

1444 *Figure 3: Liquid profiles at the output of a packed bed reactor during a*
1445 *hydrothermal extraction process: (a) TOC evolution, (b) molecular weight*
1446 *evolution (Mw) when both stages are presents and molecular weight evolution*
1447 *when only stage 2 is present.*

1448 *Figure 4: Relation between the pH and the extracted biomass.*

1449 *Figure 5: Hydrothermal extraction of eucalyptus in a semi-continuous reactor*
1450 *(solid time of 90 min): evolution of the hemicellulose extraction yield (Yield tot),*
1451 *the yield of hexoses (C6), pentoses (C5) and degradation products for eucalyptus*
1452 *with temperature (a) and residence time at 185 °C (b) [4]*

1453 *Figure 6. Effect of subcritical water temperature on the extraction of different*
1454 *phenolic compounds from defatted rice bran (residence time = 10 min). Obtained*
1455 *from Pourali et al [40]*

1456 *Figure 7. Cellulose formula*

1457 *Figure 8. Sugars yield from cellulose hydrolysis in hydrothermal medium along*
1458 *reaction time. Experiment temperature: red = 400°C; yellow = 350 °C; blue =*
1459 *300°C. Experiment pressure (♦) 27 MPa; (■) 25 / 23 MPa and (▲) 23 / 18 MPa*
1460 *[76].*

1461 *Figure 9. Reaction pathway for cellulose hydrolysis in supercritical water based*
1462 *on [71].*

1463 *Figure 10. Kinetic constants Arrhenius fitting for fructose dehydration to 5-HMF*
1464 *at 25 MPa and temperatures between 300 and 400°C [76]. a) Kinetic evaluation*
1465 *just considering cellulose and derived products concentration. b) Kinetic*
1466 *evaluation also considering protons and hydroxide ions concentrations as*
1467 *reagents.*

1468 *Figure 11. Kinetic analysis for cellulose concentrations of 5, 15 and 20 % w/w*
1469 *(corresponding to 1.5, 4.5 and 6 % w/w at the reactor inlet). The regression*
1470 *coefficients were: 0.90, 0.81 and 0.96, respectively [71].*

1471 *Figure 12. Typical structure of lignin derived from hardwood (left) and softwood*
1472 *(right) [87]*

1473 *Figure 13. Proposed scheme for degradation of lignin under near and*
1474 *supercritical condition*

1475

1476 Appendix 1. Solid and liquid residence time

1477

1478 During an extraction or reaction process where a packed bed reactor is involved (Figure S1) two
1479 different residence times can be defined, one for the solid and another one for the liquid. The
1480 solid residence time corresponds to the amount of time spent during the operation since it is
1481 fixed inside the reactor. For instance, the solid residence time in the work of *Cabeza et al.* [1]
1482 was 94 min because they treated 5 g of *holm oak* with hot pressurized water during 94 min. In
1483 contrast, the liquid is continuously flowing through the reactor. Therefore, the liquid residence
1484 depends on the reactor volume (V), the reactor porosity (ϵ) and the volumetric flow (Q) fed,
1485 being this time defined as $V \cdot \epsilon / Q$. For this reason, it was between 2 and 15 min in the work of
1486 *Cabeza et al.* [1] since each experiment was done with a different volumetric flow.

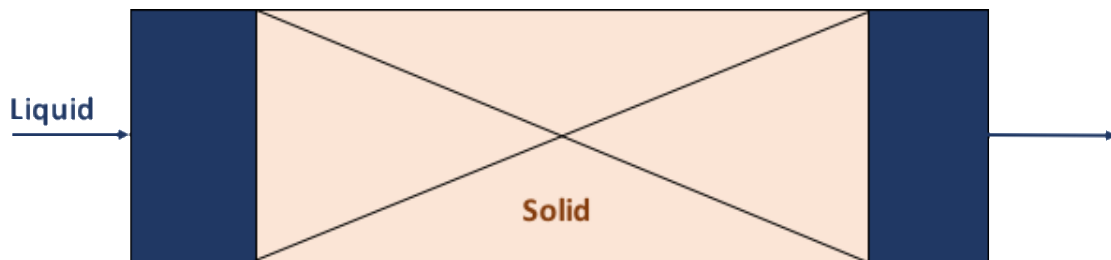
1487

1488 To sum up, the solid residence time refers to the time that the solid is being treated with the
1489 liquid. And the liquid residence time is the time that the liquid is inside the reactor.

1490

1491

1492



1493

1494

1495

Figure S1: packed bed reactor scheme

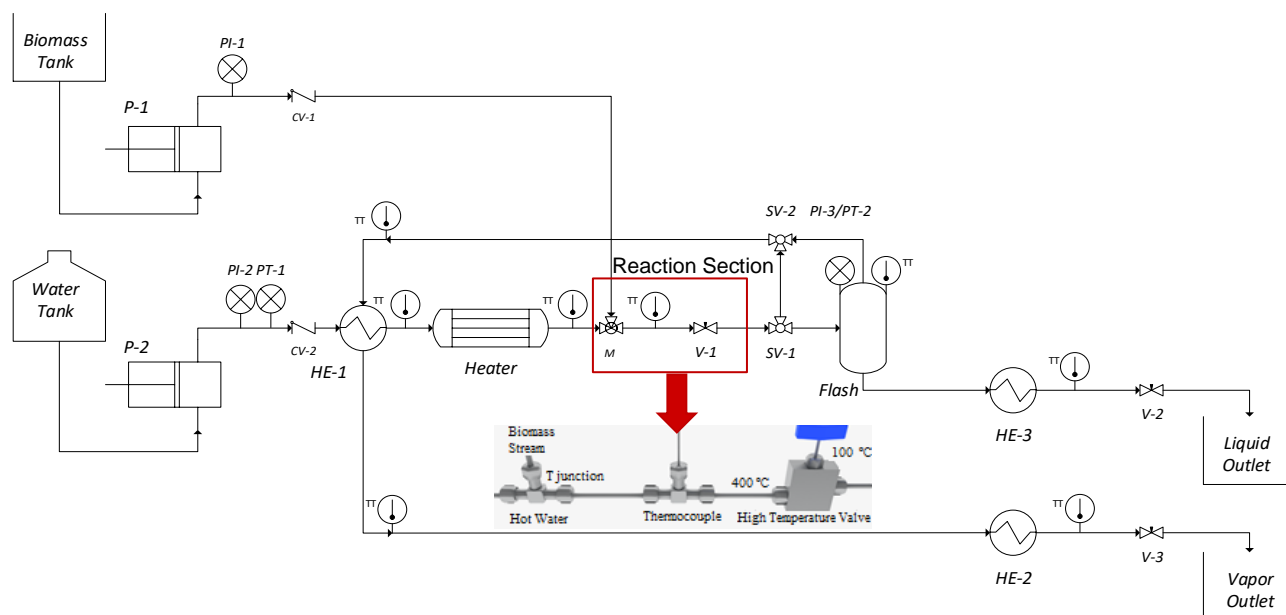
1496

1497 [1] A. Cabeza, F. Sobrón, F.M. Yedro, J. García-Serna, Two-phase modelling and simulation
1498 of the hydrothermal fractionation of holm oak in a packed bed reactor with hot
1499 pressurized water, *Chem. Eng. Sci.* 138 (2015) 59–70.
1500 doi:<http://doi.org/10.1016/j.ces.2015.07.024>.

1501

1502

1504



1505

1506 Figure S2. Experimental set-up where a micro-reactor was used to hydrolyze cellulose and biomass at
 1507 supercritical water conditions [1].

1508

1509 The results of cellulose and biomass hydrolysis in supercritical water discussed in the main
 1510 manuscript [1–7] were performed in the continuous plant of the FASTSUGARS process, able to
 1511 hydrolyze biomass in SCW at temperatures up to 400 °C and pressures up to 30 MPa. A scheme
 1512 of the experimental set-up designed by the High Pressure Processes Group is shown in Figure
 1513 S2.

1514 Briefly, water and a biomass suspension were continuously pumped to the reactor at the operating
 1515 pressure (25 MPa). At the inlet of the reactor (as a tee junction-M-) the biomass was
 1516 instantaneously heated up by mixing it with a SCW stream, reaching in that way the operating
 1517 temperature (400 °C). After the desired reaction time was achieved, the reactor effluent was
 1518 suddenly depressurized through a high temperature valve (V-1) obtaining an instantaneous
 1519 cooling and therefore, stopping the reactions. The cooling method was an important part of the
 1520 FASTSUGARS process, because it was the mechanism used to effectively stop the reactions,
 1521 avoiding uncontrolled reactions and the dilution of the products, which would occur if they were
 1522 cooled down by quenching.

1523 An electric heater was used to control the temperature of the water stream with an adjustable
 1524 power up to 10 kW. Also, a heat exchanger (HE-1) was used to both preheat the water stream
 1525 and cool down the product, introducing in that way a heat integration system. SCW was supplied
 1526 up to a maximum flow rate of 5 kg/h by pump P-2 and biomass suspension was fed to a maximum
 1527 flow rate of 3 kg/h by pump P-1.

1528 Finally, a flash chamber separator was installed after the reactor, allowing the separation of the
 1529 products into two phases: a vapor phase mainly composed of water and a liquid phase with the
 1530 concentrated product. After this stage, two heat exchangers were used to cool down the sample
 1531 to room temperature (HE-2 and HE-3).

1532

1533 [1] C.M. Martínez, D.A. Cantero, M.D. Bermejo, M.J. Cocero, Hydrolysis of cellulose in
 1534 supercritical water: reagent concentration as a selectivity factor, *Cellulose*. 22 (2015)
 1535 2231–2243. doi:10.1007/s10570-015-0674-3.

1536 [2] D.A. Cantero, M.D. Bermejo, M.J. Cocero, Governing Chemistry of Cellulose Hydrolysis
 1537 in Supercritical Water, *ChemSusChem*. 8 (2015) 1026–1033.
 1538 doi:10.1002/cssc.201403385.

- 1539 [3] D.A. Cantero, M.D. Bermejo, M.J. Cocero, Kinetic analysis of cellulose depolymerization
1540 reactions in near critical water, *J. Supercrit. Fluids*. 75 (2013) 48–57.
1541 <http://www.sciencedirect.com/science/article/pii/S0896844612003841>.
- 1542 [4] D.A. Cantero, Á. Sánchez Tapia, M.D. Bermejo, M.J. Cocero, Pressure and temperature
1543 effect on cellulose hydrolysis in pressurized water, *Chem. Eng. J.* 276 (2015) 145–154.
1544 doi:10.1016/j.cej.2015.04.076.
- 1545 [5] D.A. Cantero, M. Dolores Bermejo, M. José Cocero, High glucose selectivity in
1546 pressurized water hydrolysis of cellulose using ultra-fast reactors, *Bioresour. Technol.*
1547 135 (2013) 697–703. doi:10.1016/j.biortech.2012.09.035.
- 1548 [6] D.A. Cantero, C. Martínez, M.D. Bermejo, M.J. Cocero, Simultaneous and selective
1549 recovery of cellulose and hemicellulose fractions from wheat bran by supercritical water
1550 hydrolysis, *Green Chem.* 17 (2015) 610–618. doi:10.1039/c4gc01359j.
- 1551 [7] A. Romero, D.A. Cantero, A. Nieto-Márquez, C. Martínez, E. Alonso, M.J. Cocero,
1552 Supercritical water hydrolysis of cellulosic biomass as effective pretreatment to catalytic
1553 production of hexitols and ethylene glycol over Ru/MCM-48, *Green Chem.* 18 (2016)
1554 4051–4062. doi:10.1039/C6GC00374E.
1555